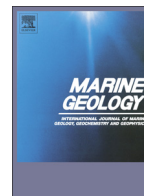




Contents lists available at ScienceDirect

Marine Geology

journal homepage: www.elsevier.com/locate/margeo

Origin of the large Pliocene and Pleistocene debris flows on the Algarve margin

E. Ducassou^{a,*}, L. Fournier^a, F.J. Sierro^b, C.A. Alvarez Zarikian^c, J. Lofi^d, J.A. Flores^b, C. Roque^e

^a Université de Bordeaux, UMR CNRS 5805 EPOC, Allée Geoffroy St Hilaire, 33615 Pessac cedex, France

^b Grupo de Geociencias Oceanicas, Universidad de Salamanca, Spain

^c International Ocean Discovery Program, Texas A&M University, College Station, TX, USA

^d Géosciences Montpellier, Montpellier, France

^e IPMA, Divisão de Geologia Marinha e Georrecursos, Lisbon, Portugal

ARTICLE INFO

Article history:

Received 11 February 2015

Received in revised form 20 July 2015

Accepted 27 August 2015

Available online xxxx

Keywords:

Debrite

Algarve margin

Plio-pleistocene

Foraminiferal assemblages

Ostracods

Erosion

ABSTRACT

The base of the Faro contouritic drift (IODP Site U1386) on the northern margin of the Gulf of Cádiz (Algarve margin) is characterized by two sequences of frequent gravity deposits with different ages and compositions. Among these gravity deposits, several relatively thick debrites (up to 12 m) have been observed and studied in detail.

Sedimentological analyses have been performed and because of non-turbulent behavior of debris flows, detailed micropaleontological studies could be realized. Planktonic foraminifera thus allowed establishing a detailed biostratigraphy of these deposits. Benthic foraminifer and ostracod assemblages were used to evaluate the origin of the sediment composing these debris flows and estimate their run-out distance.

These debrites are dated from Early Pliocene and early Pleistocene, and were deposited in a mesobathyal environment. They comprise silty mud clasts and matrixes with sand content up to 34%. The Early Pliocene debrites are bioclast-rich whereas the Early Pleistocene debrite is enriched in terrigenous particles. The data indicates that these debrites were triggered on the continental shelf and traveled less than 100 km, eroding the seafloor all along their path for the Early Pliocene debrites and only the first part of their path for the early Pleistocene debrite. Matrixes originate from failure areas whereas eroded sediments along the flow pathway are incorporated into the flow as clasts.

High abundance of shelf fauna during the Early Pliocene and great supply of terrigenous particles from rivers during the early Pleistocene in the south-western Iberian margin have favored gravity flows from the continental shelf to the slope. The contouritic paleo-moat of the Faro drift has been a determining channeling feature for gravity flows along the Algarve margin during the early Pleistocene, testifying of the strong interaction between MOW circulation and down-slope processes. Tectonic and diapiric activities were significant during Early Pliocene and early Pleistocene on the Algarve margin and could have been triggering parameters of failures related to these debris flows.

© 2015 Elsevier B.V. All rights reserved.

1. Introduction

The contouritic Faro Drift is one of the largest drifts of the Gulf of Cádiz and has been regularly used as a reference for studies of contourite deposits (e.g. Gonthier et al., 1984; Faugères et al., 1985; Hernández-Molina et al., 2006; Fig. 1). During the Integrated Ocean Drilling Program (IODP) Expedition 339 *Mediterranean Outflow*, thick and numerous gravity deposits have been observed at two sites drilled into the Faro Drift (U1386 and U1387) at the base of the contouritic deposits (Expedition 339 Scientists, 2013; Hernández-Molina et al.,

2013, 2014). These gravity deposits are mainly turbidites but also thick debrites (mostly U1386) and some slumps (mostly U1387). The preliminary stratigraphy established onboard indicated that these gravity deposits are coeval with the onset of *Mediterranean Outflow Water* (MOW) (Hernández-Molina et al., 2014). The oldest gravity deposits occurred during the Early Pliocene (~5.2–4.5 Ma; called unit I in this work; Fig. 2) and correspond to typical sedimentation on a continental slope with alternation of terrigenous turbidites, small slumps, contourites and significant hemipelagites. This period of mixed downslope and along-slope deposition has been essentially recorded in the lowest part of Site U1387 (Expedition 339 Scientists, 2013; Hernández-Molina et al. 2013, 2014). At first description, sediment composition during this period seem similar to the one observed in the overlying thick contouritic sequence of the Faro Drift.

* Corresponding author.

E-mail address: e.ducassou@epoc.u-bordeaux1.fr (E. Ducassou).

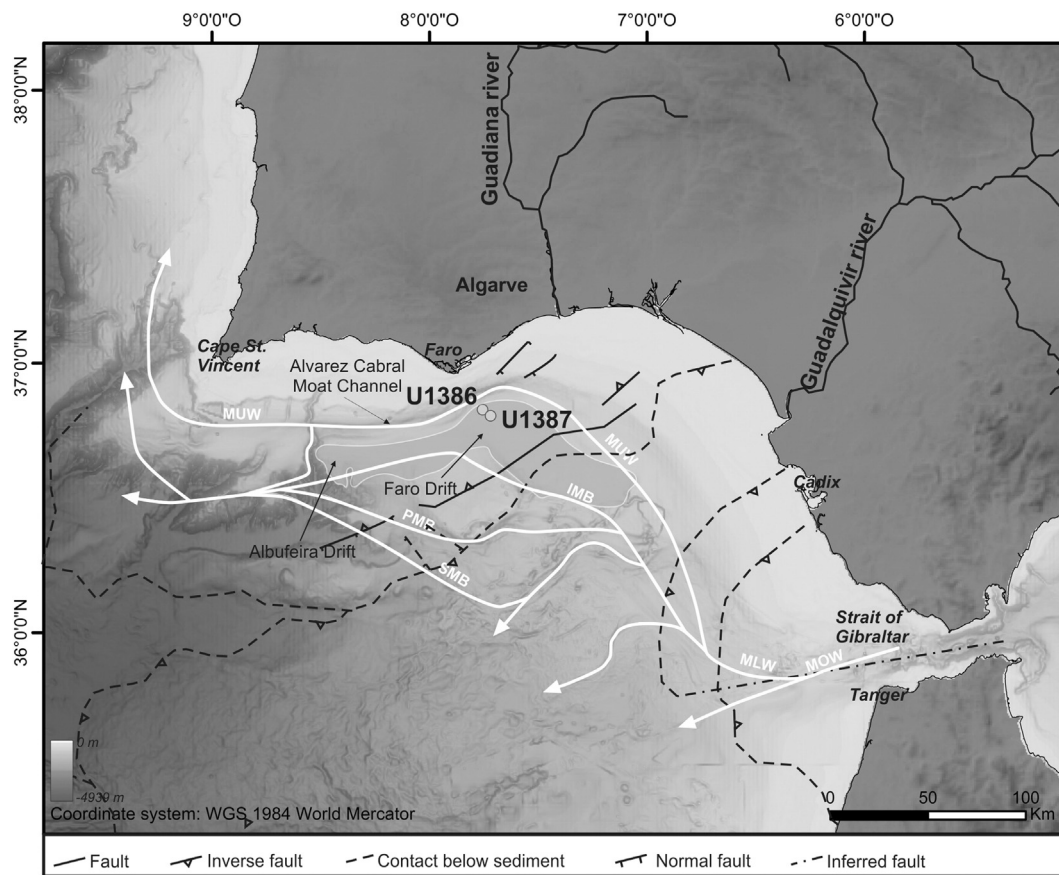


Fig. 1. Bathymetric map of the Gulf of Cádiz showing the location of IODP Sites U1386 and U1387. The Faro Drift extension is represented in gray with a white contour. MOW pathways are indicated by the white arrows. Black dashed lines correspond to olistostrome edges described by Iribarren et al. (2009). MOW: Mediterranean Outflow Water. MUW: Mediterranean Upper Water. MLW: Mediterranean Lower Water. IMB: Intermediate MOW Branch. PMB: Principal MOW Branch. SMB: South MOW Branch.

A second phase of gravity deposits has been described between ~5.2 and 3.5 Ma (units I and II in this work; Fig. 2). It has been distinguished from the previous one because reworked sediments are enriched in bioclasts and gravity deposits are dominant. This unit is characterized by alternation of turbidites, thick debrites and hemipelagites and has been mainly observed at Site U1386. It is coeval with the onset of limited MOW circulation (Hernández-Molina et al. 2013, 2014). The most recent sequence of gravity deposits is dated between 1.66 and 1.25 Ma (unit III in this work; Fig. 2). It is composed of mainly terrigenous particles and gravity deposits are greatly dominant.

This work focuses on Site U1386, in particular two geological periods (4.5–3.5 Ma and 1.66–1.25 Ma) during which sedimentation on the Algarve margin was very different from the present, dominated by downslope activity and under the influence of various sediment sources. This study examines the micropaleontological composition of debrites. This was made possible because, due to their transport mechanism, debris flows have a better preservation potential for the delicate tests and shells of microfossils than turbulent flows. Cohesion of the fine-grained matrix indeed prevents erosion and vertical/horizontal mixing of particles from clasts and matrix (Mulder and Alexander, 2001). Moreover, some debrites observed at Site U1386 are particularly thick (up to 12 m) and are thus significant in the history of the Algarve margin sedimentation.

Debris flows have been largely studied and previous works show that they are related to sediment failures, their volume could be greatly variable, the thinnest debris flows could be highly mobile (Schwab et al., 1996; Migeon et al., 2010; Ducassou et al., 2013), involving mechanisms such as hydroplaning (Mohrig et al., 1998), elevated basal pore-fluid pressures (Major and Iverson, 1999) or a sandy sole (Haughton et al.,

2003), and erosion is not systematic along their pathway (Schwab et al., 1996; Carter, 2001; Lastras et al., 2004; Ducassou et al., 2013). Debrite volumes could thus illustrate only the volume of the failed area or this volume could be added to the volume of sediment eroded at the sea floor along their pathway. Studying debrites with a compositional approach allows better identifying failure and instable areas and estimating potential sea floor erosion during the flow in terms of run-out distance (benthic microfossil assemblages) and thickness of eroded sediment (biostratigraphical investigation).

Methods used in this study are almost the same than those used and described by Ducassou et al. (2013). This methodology involves a study of planktonic and benthic foraminifera, and benthic ostracods in both clast and matrix samples.

The main goal of this work is to understand the 4.5–3.5 Ma and 1.66–1.25 Ma depositional units during which sedimentation of the Algarve margin was dominated by gravity deposits, contemporaneously to the MOW onset. The second goal is to show how drill cores can be used to reconstruct the flow behavior of debris flows. To answer these objectives, content of each debris flow event was analyzed in order to determine age(s) and source(s) of the reworked sediments.

2. Geological setting of the Algarve margin

The Algarve margin is located in the northern part of the Gulf of Cádiz (Fig. 1). As other continental margins of the Gulf of Cádiz, it is characterized by a concave morphology: the continental shelf, reaching 140 m water depth, is relatively narrow with a mean width of 20 km. The continental slope is the greatest domain (Hernández-Molina et al., 2006). The upper slope, between 140 and 400 m water depth, has a

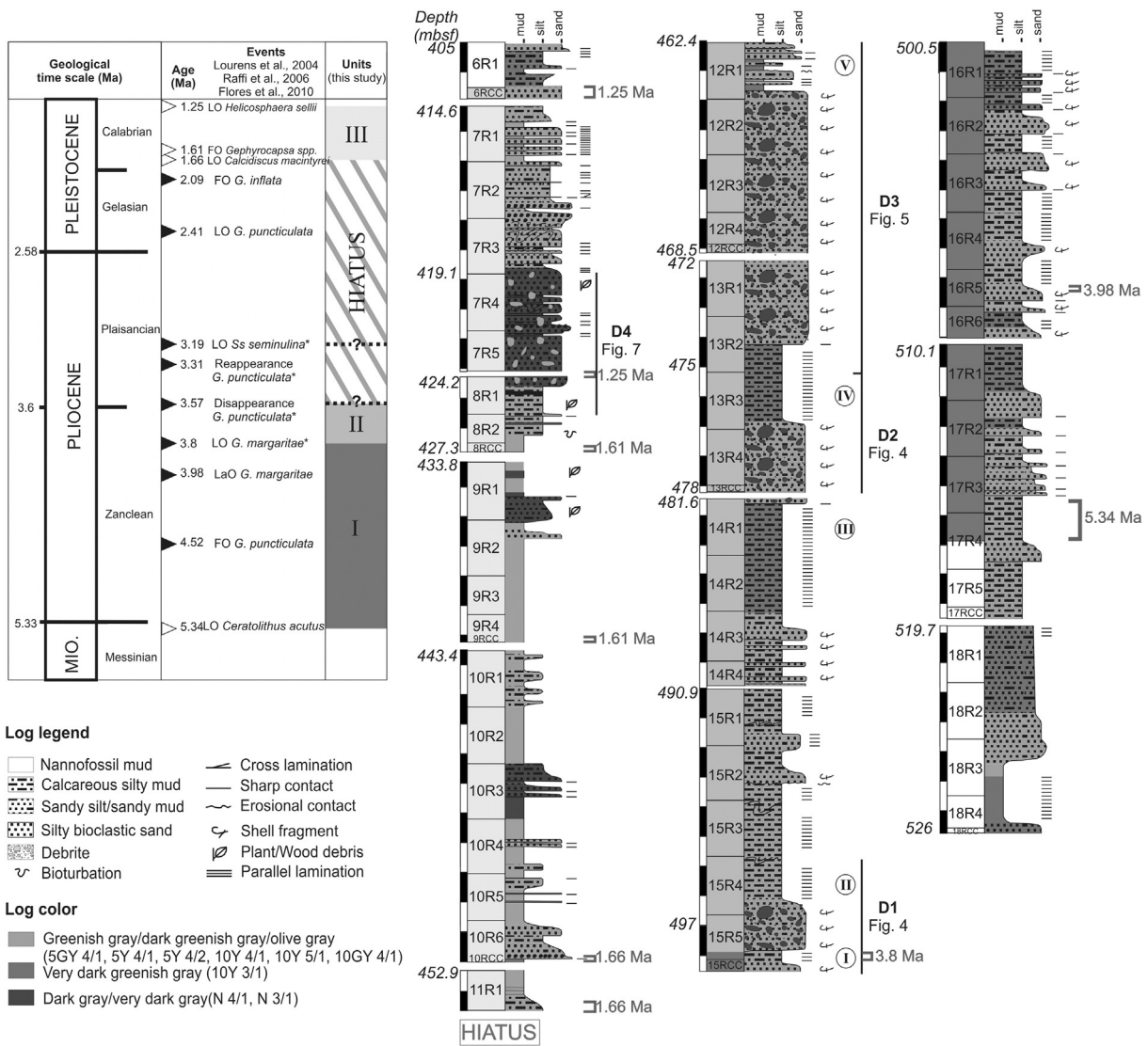


Fig. 2. [Left]: biostratigraphy based on planktonic foraminifer events of Lourens (2004) and calcareous nannofossils (Raffi et al., 2006; Flores et al., 2010). FO: first occurrence; LO: last occurrence; LaO: last abundant occurrence. The asterisk (*) indicates new events used in this study to refine the base of the hiatus and differentiate units I and II. [Right]: lithological log of Site U1386, Hole C with depths in meters below sea floor (mbsf) and ages established on board and during this study. Roman numerals I to V correspond to samples collected in hemipelagic sediments. D1 to D4 indicate the four debris described in this work.

mean width of 10 km. The middle slope, between 400 and 1200 m water depth, is characterized by a wide terrace morphology up to 100 km-wide, and the lower slope, between 1200 and 4000 m water depth, is about 50 km-wide (Hernández-Molina et al., 2006). The present morphology and near-surface deposits of the middle slope of the Algarve margin have been controlled by the MOW. Following the opening of the Strait of Gibraltar, along-slope processes resulting from the bottom current activity have dominated the middle slope since the middle of the Pliocene (3.5–3.2 Ma), building up the Faro Drift (Nelson et al., 1993; Maldonado and Nelson, 1999; Maldonado et al., 1999; Llave et al., 2006; Hernández-Molina et al., 2014).

The Algarve margin is also located close to the Africa–Eurasia plate boundary (Zitellini et al., 2009). A compressional regime occurred from the Late Cretaceous through the Paleogene, related to Africa–Eurasia convergence. During the Miocene, this collision associated to a westward drift led to the formation of the Rif and Betic orogen and the emplacement of significant allochthonous masses in the Guadalquivir and Rharrb basins and in the Gulf of Cádiz (olistostrome; Torelli et al., 1997; Maldonado et al., 1999; Medialdea et al., 2004 among others; Fig. 1). Emplacement of this olistostrome created instabilities initiating

diapiric processes (salt and marls) and Betic-Rif orogen load generated flexural subsidence in the Algarve margin (Maldonado and Nelson, 1999). Subsidence decreased at the end of the Early Pliocene and more stable conditions dominated the Algarve during the Late Pliocene and Quaternary, except ongoing diapiric and fault activity (Nelson et al., 1993, 1999; Maldonado et al., 1999; Medialdea et al., 2004; Llave et al., 2006; Hernández-Molina et al., 2006; Roque et al., 2012). Significant sea-level changes during the Late Pliocene and Quaternary allowed high terrigenous supplies through the two main rivers from Iberia: the Guadalquivir and Guadiana rivers (Maldonado and Nelson, 1999; Fig. 1). The Betic corridor was a deep flexural basin connecting the Tethys and the Atlantic oceans during the Middle Miocene (Riaza and Martinez del Omo, 1996). This connection was shut down during the Late Miocene, creating intracontinental basins and one marine basin: the Guadalquivir basin (Ledesma, 2000). This marine basin evolved toward a shallow flexural basin and a continental basin (foreland) up to the Early Pleistocene (Iribarren et al., 2009). During the Plio-Quaternary period, sedimentary supplies related to erosion of the Rif and Betic ranges correspond to ~35,000 km³ of sediment dumped into the Gulf of Cádiz (Iribarren et al., 2009).

3. Material and methods

3.1. IODP site U1386

The Site U1386 drilled in the Faro Drift (36°49.685 N, 7°45.321 W) is located at mid slope (565 m) ~25 km at the south-south-east of Faro (Fig. 1). Three holes (A, B and C) were drilled and cored at this site by the scientific ocean-drilling vessel *JOIDES Resolution* in November 2011. Holes U1386A and U1386B were cored to a total depth of 350 m below the sea floor (mbsf) and Hole U1386C was drilled without coring

to 300 mbsf and then rotary-cored to 526 mbsf (13 cores with a recovery of 58.5%; Fig. 3). Onboard, these cores were divided into sections of 1.5 m length. The present work focuses on the sedimentary section recovered from Hole U1386C that extends from the Miocene to the Pleistocene age, and especially the interval between 400 and 500 mbsf. This ~100 m-thick sedimentary sequence is characterized by gravity deposits interbedded with contourite and hemipelagite deposits. Gravity deposits include turbidites with varying thicknesses (cm to dm) and debrites, occasionally relatively thick (1 m to >10 m). Debrites are studied in this work because of the good preservation of biogenic material.

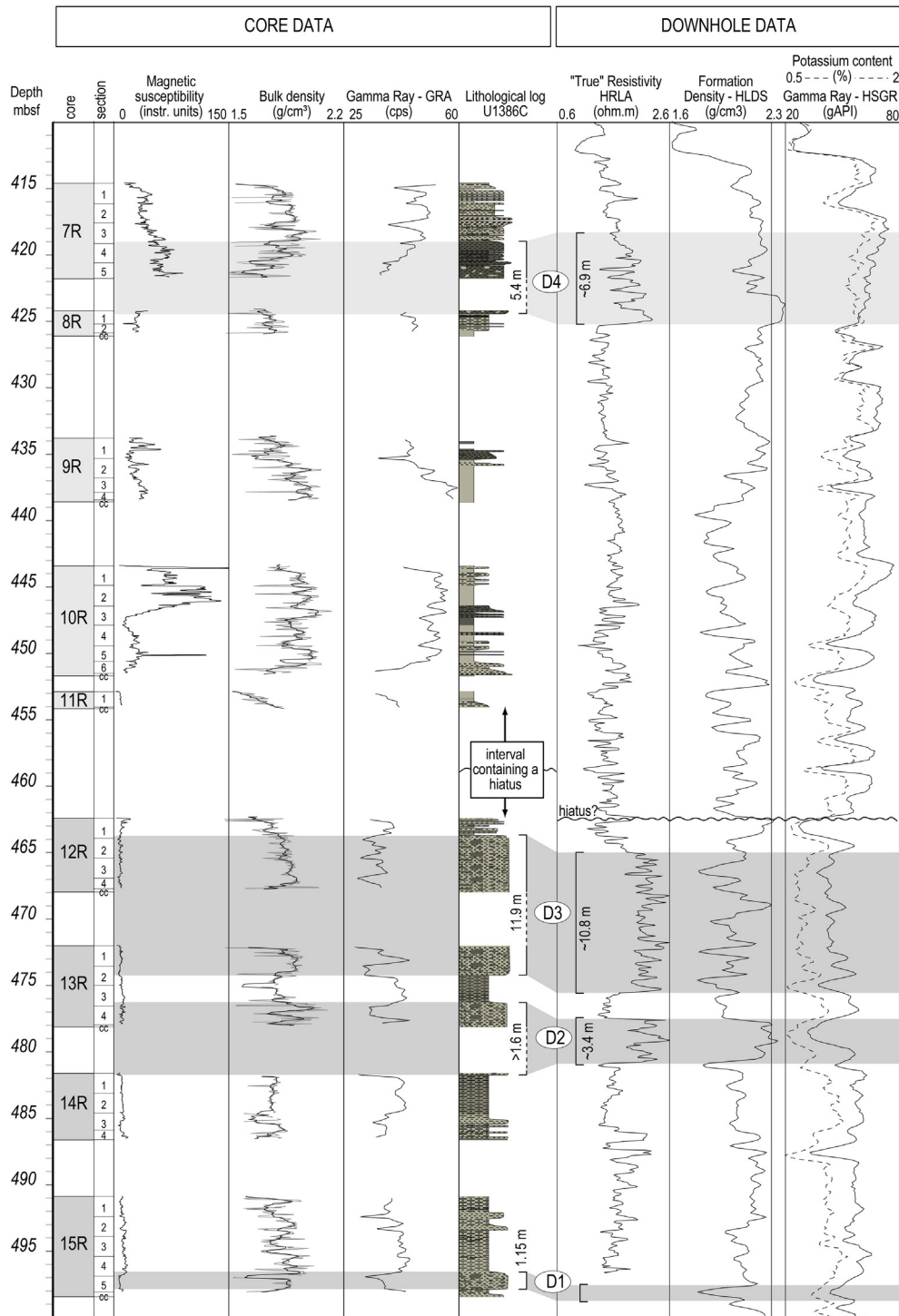


Fig. 3. Shipboard petrophysical measurements performed on whole-round core sections (gamma ray attenuation (GRA), bulk density, and magnetic susceptibility), lithological log and downhole logs (resistivity (HRLA), density (HLDS) and natural gamma ray (HSGR) logs). D1 to D4 indicate the four debrites described in this work.

Four debrites are observed in 5 cores with thicknesses from 1.15 m to ~11 m (Figs. 2 and 3). These thicknesses will be discussed below as, except for the oldest debrite, recovery of debrites is poor (Fig. 3). For these four debrites, clasts and matrix were easy to distinguish (e.g. texture, color, and lithology) and sampling locations were decided according to various lithologies of clasts to be the most representative and available quantity of sediment, especially in clasts. The smallest clasts with diameters <2 cm have not been sampled, inducing a potential bias in results. Sampling (~5–10 cm³) has been made carefully in clasts and in matrixes forming each debrite, and in hemipelagic intervals in-between debrites. The goal being to identify composition and sources of each clast and each matrix, it was important to avoid mixing of clast and matrix sediment during sampling. Thirty-six samples have been collected and analyzed from Hole U1386C: 7 samples were taken in hemipelagic sediments (above and below debrites), 12 in matrixes (10 in the Early Pliocene and 2 in early Pleistocene debrites) and 17 in clasts (15 in the Early Pliocene and 2 in the early Pleistocene debrites).

3.2. Sedimentological analyses

Debrites have been identified from lithological descriptions done and photos taken during Expedition 339, with typical textural features such as mud clasts floating in a matrix. Grain size of each sample has been measured with a laser microgranulometer MALVERN MASTERSIZER S (University of Bordeaux, EPOC laboratory). Each sample has been sieved at 63 and 150 µm, and the mineral fraction has been analyzed under a microscope. For each sample, a minimum of 300 particles has been counted. Mineral content illustrated in the following figures is in the sediment size fraction >150 µm. For some samples, thin sections have been made with grains picked from the >150 µm fraction to better identify the mineralogical composition (detrital fraction: quartz, micas, lithic fragments, etc., and authigenic fraction: aggregates, gypsum, pyrite and glauconite).

3.3. Micropaleontological analyses

Analyses of planktonic and benthic foraminifera and benthic ostracoda have been performed mainly in the sediment fraction >150 µm only on 25 samples from debrites D3 and D4 (Figs. 2 and 3) and in hemipelagic sediments as the thickness of D1 would not be representative and the missing part of D2 is larger than the recovered part. The fraction 63–150 µm also has been checked for ostracods. Samples have been analyzed under a microscope. Identification and counting of foraminifera have been made on split samples comprising at least 300 specimens of planktonic and 300 specimens of benthic foraminifera. Because ostracods were less abundant than foraminifers in the samples, all ostracods were counted and identified. Microfaunal counts are given in the figures in percentage of the total assemblage.

Taxonomy of planktonic foraminifera is based on Kennett and Srinivasan (1983). Planktonic foraminifera were examined to refine the biostratigraphy established onboard during Expedition 339 with calcareous nannofossils (Raffi et al., 2006; Flores et al., 2010; Expedition 339 Scientists, 2013). The planktonic events used in this work are those described by Lourens (2004). The new stratigraphical results are summarized in Table 1 and indicated with asterisks in Fig. 2.

Taxonomy of benthic foraminifera is based on the works by Van Morkhoven (1986); Jones and Brady (1994); Cimerman and Langer (1991); Dayja (2002) and Alves Martins and Ruivo Dragão Gomes (2004). Taxonomy of ostracoda is based on the works of Bonaduce et al. (1975); Ruiz and Gonzalez-Regalado (1996); Ruiz-Muñoz et al. (1998), and Faranda and Gliozzi (2008). Benthic foraminifera and ostracoda are used to identify paleoenvironments (depth in sediment, available food, hydrodynamism, oxygenation, and paleobathymetry; Jorissen et al., 1995; Boomer et al., 2003; Ruiz et al., 2008; Rodriguez-Lazaro and Ruiz-Muñoz, 2012). Distribution of benthic foraminifera and ostracoda essentially depends on bottom water

oxygenation and trophic level of the environment (Jorissen et al., 1995; Rodriguez-Lazaro and Ruiz-Muñoz, 2012). These parameters vary with bathymetry in such a way that there is a close relation between the benthic microfaunal assemblages and water depth.

This work focuses mainly on life depth of benthic foraminifera and ostracoda that have a proportion > 5%, in order to estimate the triggering paleodepths of debrites (failed sediment), their run-out distance and possible associated erosion (sediment eroded along the flow pathway). In the following figures, distribution of benthic foraminifer species in the Gulf of Cádiz related to water depth is based on present and past distributions presented in the works of Lutze (1986); Mathieu (1986); Van Morkhoven (1986); Jones and Brady (1994); Levy et al. (1995); Kouwenhoven (2000); Dayja (2002); Alves Martins and Ruivo Dragão Gomes (2004), and Mendes et al. (2004), taking into account the presence of the Mediterranean Upper Water circulation (Fig. 1). The following bathymetrical zonation is used: inner shelf (0–100 m), outer shelf (100–200 m), epibathyal (200–600 m), mesobathyal (600–1000 m), infrabathyal (1000–2000 m) and abyssal (>2000 m).

Results obtained with life depths of benthic foraminifera are compared to Van der Zwaan et al.'s (1990) and Wright and Berggren's (1977) that allow calculating paleodepths. Van der Zwaan et al.'s (1990) has been successfully tested on sediments from the Gulf of Mexico, Gulf of California, western coast of United-States, eastern Mediterranean and the Adriatic Sea (Van der Zwaan et al., 1990; De Rijk et al., 1999). Dayja (2002) applied Wright and Berggren's (1977) in sediments from the Rif corridor in Morocco (south of Gulf of Cadiz). As the Van der Zwaan et al.'s equation has not been tested in the Gulf of Cadiz; both equations are used in this work. They both use the planktonic foraminifer proportion (%P) to calculate the paleodepths. In Wright and Berggren's (1977), %P = P*100/(P + B) where P is the planktonic foraminifer number and B is the benthic foraminifer number. Wright and Berggren's (1977):

$$\text{Depth} = e^{(0.0418\%P + 3.4823)}$$

In Van der Zwaan et al. (1990), %P = (100*P)/(P + B-S) where P is the planktonic foraminifer number, B is the benthic foraminifer number and S is the number of deep endofaunal benthic foraminifera (*Bolivina* spp., *Bulimina* spp. except *costata*, *Uvigerina* spp., *Valvulineria* spp., *Cancris* spp., *Chilostomella* spp., *Globobulimina* spp., *Rectuvigerina* spp., *Stainforthia* spp. and *Fursenkoina* spp.; Van der Zwaan et al., 1990; Van der Zwaan and Jorissen, 1991; Rathburn and Corliss, 1994; Fariduddin and Loubère, 1997; Jorissen and Wittling, 1999; Van Hinsbergen et al., 2005). Van der Zwaan et al.'s (1990):

$$\text{Depth} = e^{(3.58718 + (0.03534\%P))}$$

At 1200 m of water depth (%P = 99), the 90% confidence limit ranges from 860 to 1650 m.

The results are used to estimate possible triggering depths of debrites. Thanks to comparison between components of debrite samples and reference samples (hemipelagic sediments) which indicate depositional environment characteristics at site location in between gravity flows, it is possible to estimate the run-out distance of debris flows.

In marine gravity flows such as turbidity currents or debris flows, particles are easily transported from shallow to deep environments, most of the time altering biogenic particles. In debris flows, clasts are theoretically well preserved from mixing and mechanical erosion because of cohesion of matrix (non-turbulent flow). If the failure area is characterized by gravity sedimentation such as turbidity currents, clasts could be representative of past gravity deposits, reworked in a debris flow. It is a point to keep in mind for paleodepth estimation because benthic foraminifera can be easily displaced and the debrites studied in this work are interbedded with numerous turbidites.

Table 1

Abundance of planktonic foraminifers in Hole U1386C. P = present (<1%); R = rare (1–5%); F = few (>5–10%); A = abundant (>10–30%).

| Samples | Cores/Sections | Depth (mbsf) | Dentoglobigerina altispira | Dentoglobigerina baroemoensis | Globigerina apertura | Globigerina bulloides | Globigerina calida | Globigerina obesa | Beella digitata | Globigerinella aequilateralis |
|------------------------------|----------------|--------------|----------------------------|-------------------------------|----------------------|-----------------------|--------------------|-------------------|-----------------|-------------------------------|
| Early Pleistocene Debrite D4 | Matrix 2 | 7R4 | 419.62 | | | A | P | | | |
| | Matrix 1 | 7R5 | 420.62 | | | A | | | | |
| | Clast B | 7R5 | 420.69 | | | A | | | | |
| | Clast A | 7R5 | 421.56 | | | D | | R | | R |
| Hemipelagites V | | 12R1 | 462.65 | | F | D | | R | | |
| | Clast J | 12R1 | 463.58 | | A | D | P | P | P | |
| | Matrix 6 | 12R1 | 463.73 | | A | D | | | | |
| | Clast I | 12R2 | 464.13 | | A | A | | P | | P |
| Early Pliocene Debrite D3 | Matrix 5 | 12R2 | 464.33 | | A | A | | | | R |
| | Clast H | 12R2 | 464.5 | R | A | A | | P | | |
| | Clast G | 12R2 | 464.64 | | A | A | | P | | P |
| | Clast F | 12R2 | 465.02 | | A | A | | P | | |
| | Matrix 4 | 12R2 | 465.18 | | A | D | | | | P |
| | Clast E | 12R3 | 465.52 | | P | A | D | | | P |
| | Clast D | 12R3 | 466.08 | | A | A | | | | P |
| | Clast C | 12R3 | 466.54 | | P | A | D | | | P |
| | Matrix 3 | 12R3 | 466.75 | | | F | D | | | P |
| | Clast B | 13R1 | 472.29 | | | F | D | | | P |
| | Clast A | 13R1 | 472.96 | | | F | D | | | P |
| | Matrix 2 | 13R1 | 473.4 | | | A | D | | | P |
| Hemipelagites IV | Matrix 1 | 13R2 | 474.32 | | A | D | | | | |
| | | 13R3 | 475.13 | | R | F | A | | P | |
| Hemipelagites III | | 14R1 | 481.85 | | A | A | P | R | | |
| Hemipelagites II | | 15R4 | 496.6 | R | A | A | | | | |
| Hemipelagites I | | 15R5 | 497.97 | | A | D | | R | | P |

Abundance of planktonic foraminifers, hole U1386C. P = present (<1%); R = rare (1–5%); F = few (>5–10%); A = abundant (>10–30%); D = dominant (>30%).

Table 1 (continued)

| Samples | Globigerina falconensis | Globigerinella siphonifera | Globigerinella glutinata | Globigerinoides conglobatus | Globigerinoides extremus | Globigerinoides ruber (white) | Globigerinoides immaturus | Globigerina sacculifer | Globorotalia cf. crassula | Globorotalia crassaformis s. l. | Globorotalia hirsuta (dex) | Globorotalia hirsuta (sin) |
|------------------------------|-------------------------|----------------------------|--------------------------|-----------------------------|--------------------------|-------------------------------|---------------------------|------------------------|---------------------------|---------------------------------|----------------------------|----------------------------|
| Early Pleistocene Debrite D4 | | | R | | | F | P | | | | | |
| | | | R | | | R | | | | | | |
| | | | R | | | P | | | | | | |
| | | | R | | | F | | | | | | |
| Hemipelagites V | | | R | | P | R | R | | | P | | |
| | | | F | P | R | R | R | P | | R | | |
| | | | R | | R | R | F | P | | | | |
| | | | R | | F | R | R | R | | | | |
| Early Pliocene Debrite D3 | | | R | | R | R | R | P | | P | | |
| | | | F | | R | R | R | P | | | | |
| | | | R | P | F | P | F | R | | P | | |
| | | | R | | F | R | F | R | | | | |
| | | | R | | F | R | R | P | | P | | |
| | | | R | | R | R | R | P | | | R | |
| | | | R | | F | R | F | P | | | | |
| | | | R | | F | R | R | P | | | | |
| | | | R | P | R | R | R | F | | | | |
| | | | R | | R | R | R | F | | | | |
| | | | R | | R | R | R | P | | | P | |
| | Hemipelagites IV | | F | | P | R | R | | | | R | |
| Hemipelagites III | | F | | F | P | R | | | | R | | |
| Hemipelagites II | | R | | R | P | F | P | | | R | | |
| Hemipelagites I | | R | | R | P | R | | | | | | |

Table 1 (continued)

| Samples | Globorotalia inflata (dex) | Globorotalia inflata (sin) | Globorotalia margaritae | Globorotalia menardii | Globorotalia miocenica | Globorotalia puncticulata (dex) | Globorotalia puncticulata (sin) | Globorotalia scitula (dex) | Globorotalia scitula (sin) | Globorotalia truncatulinoides (dex) | Globorotalia truncatulinoides (sin) | Globoturborotalita rubescens |
|-------------------|----------------------------|----------------------------|-------------------------|-----------------------|------------------------|---------------------------------|---------------------------------|----------------------------|----------------------------|-------------------------------------|-------------------------------------|------------------------------|
| Early Pleistocene | F | A | | P | | | | | | P | | |
| Debrite D4 | P | A | | | | | | P | | P | | |
| Hemipelagites V | | A | | | | | A | | | | | |
| | | | R | | | | A | | | | | |
| | | | P | | | | R | | | | | |
| | | | P | | | | A | | | | | |
| | | | R | | | | A | | | | | |
| | | | R | | | | A | | | | | |
| Early Pliocene | | | R | R | | | A | P | | | | |
| Debrite D3 | | | P | | | | A | P | | | | |
| | | | P | | | P | A | | | | | |
| | | | P | P | | | R | | | | | |
| | | | P | | | R | A | | | | | |
| | | | P | | | | A | | | | | |
| Hemipelagites IV | | | R | | | | R | | | | | |
| Hemipelagites III | | | | | | | D | | | | | |
| Hemipelagites II | | | | | | R | A | | | | | |
| Hemipelagites I | | | R | | | | A | | | | | |

Table 1 (continued)

| Samples | Globoturborotalita tenella | Neogloboquadrina atlantica (dex) | Neogloboquadrina atlantica (sin) | Neogloboquadrina pachyderma (dex) | Neogloboquadrina pachyderma (sin) | Orbulina universa | Sphaerodinaella dehiscens | Sphaerodinellopsis seminulina | Sphaerodinellopsis subdehiscens | Turborotalita quinqueloba | Unidentified species | Stratigraphical unit |
|------------------------------|----------------------------|----------------------------------|----------------------------------|-----------------------------------|-----------------------------------|-------------------|---------------------------|-------------------------------|---------------------------------|---------------------------|----------------------|----------------------|
| Early Pleistocene Debrite D4 | | R | | D | R | P | | | | R | P | |
| | | F | | D | P | R | | | | R | P | III |
| | | P | | D | R | R | | | | F | | |
| | | R | | A | | R | | | | F | P | |
| Hemipelagites V | | | | F | | R | | | | | | II |
| | | | | A | | F | | | | | | II |
| | | | | A | P | P | | P | | | P | |
| | | | | A | | A | | | | | P | |
| | | | | A | P | F | | R | | P | P | I |
| | | | | A | | R | | R | | | | |
| | | | | A | P | F | | R | | | | II |
| Early Pliocene Debrite D3 | | | | A | | P | | | | | P | |
| | | | | A | | R | | | | | | I |
| | | | | A | | A | | | | | | II |
| | | | | A | P | F | | P | | | | |
| | | | | A | | A | | | | | | II |
| | | | | A | P | F | | P | | | | I |
| | | | | F | | F | | P | | | | |
| | | | | F | P | A | | | | | | II |
| | | | | A | P | F | | P | | P | P | I |
| Hemipelagites IV | | | | A | | F | | P | | | | |
| Hemipelagites III | | | | P | | A | | P | | | | |
| Hemipelagites II | | | | F | | F | | R | | P | | II |
| Hemipelagites I | | | | A | | F | | P | | | P | I |
| | | | | A | | R | | | | | | I |

Taphonomic features of tests have been observed as indication of transport and environmental conditions: whole and fresh tests are typical from quiet and/or weakly oxygenated environments, pyritized tests indicate a lack of oxygen, partially broken tests or test fragments and abraded tests are related to high hydrodynamic environments or dissolution, and oxidized and black tests indicate redox conditions inside sediment (Stefanelli, 2004).

3.4. Downhole logging and core petrophysics

A set of petrophysical measurements has been performed on whole-round core sections during the IODP Expedition 339 (Hernández-

Molina et al., 2013). Among them, gamma ray attenuation (GRA) bulk density and magnetic susceptibility were measured at high resolution with a Whole-Round Multisensor Logger. Natural gamma radiation (NGR) core logs were acquired with a Natural Gamma Radiation Logger (NGRL).

Downhole logs were acquired in Hole U1386C (Hernández-Molina et al., 2013). They can be used to determine the in situ properties (physical, chemical, and structural) of the formation penetrated by a borehole. Log and core data complement one another and may be interpreted jointly. In this study, the resistivity (HRLA), density (HLDS) and natural gamma ray (HSGR) logs were used to characterize the drilled formation where core recovery was incomplete (Fig. 3).

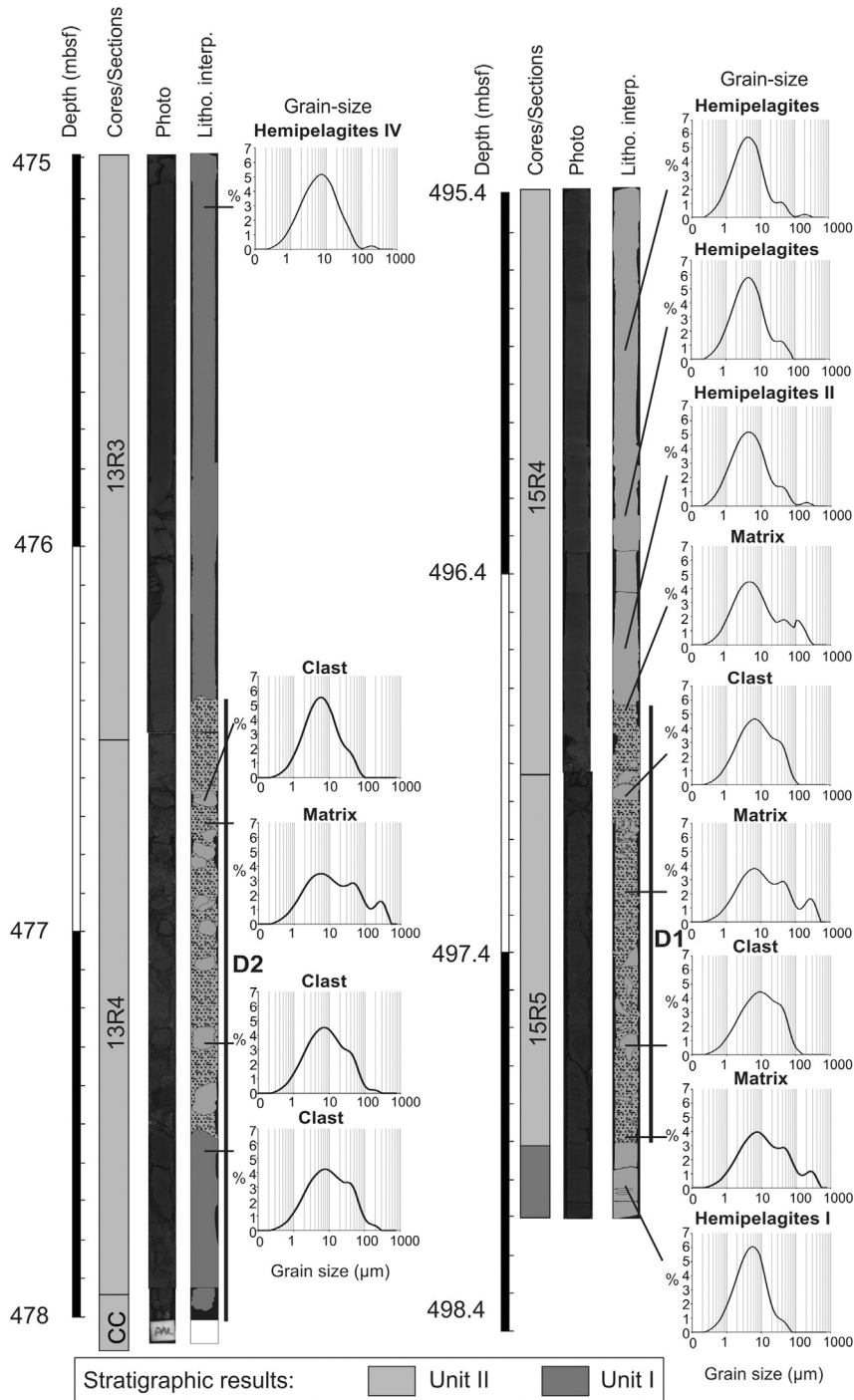


Fig. 4. Lithology and stratigraphy of the two oldest debris of the early Pliocene (D1 and D2). Sample location, grain-size results, composition of the sandy fraction and age of each sample are shown. Stratigraphic units are indicated in cores/sections box.

4. Results

4.1. Stratigraphy of debrites and associated turbidites

Five samples have been collected in hemipelagic sediments in Cores 15R to 12R from Hole U1386C and analyzed to identify the environment in which the debrites were deposited. These samples are characterized by a laminated silty clay facies with a clay content ranging from 40% to 60% and a sand content from 0.5% to 6% (Figs. 4 and 5). Composition of the fraction > 150 μm is relatively homogenous in the different samples with 45–65% of foraminifera, 5–30% of pyrite, gypsum and siliceous aggregates.

Thanks to the new investigation of planktonic foraminifer events, three stratigraphical units have been defined for this work and duration of a hiatus has been refined based on planktonic foraminifera and calcareous nannofossils (Expedition 339 Scientists, 2013 and this study; Fig. 2 and Table 1). The new biostratigraphical events identified are indicated with asterisks in Fig. 2 and involve the distinction between units I and II, and the age of the hiatus base. Unit I (5.34–3.8 Ma, in dark

gray in Fig. 2; Table 1), extending from 515.16 to 497.97 mbsf, is characterized by the presence of planktonic foraminifer species *G. margaritae* and, at its base, by the last occurrence of *Ceratolithus acutus* (calcareous nannofossil). Unit II (3.8 – >3.57 Ma in gray; Fig. 2), extending from 497.97 to 462.4 mbsf, is related to the presence of *G. punctulata* and the absence of *G. margaritae* (Table 1). Units I and II are separated from unit III by the presence of a hiatus. This hiatus, located somewhere between 454.08 and 462.87 mbsf on the core data, is at least 1.4 My long (Expedition 339 Scientists, 2013 and this study). This hiatus is tentatively placed at 462.4 mbsf based on the downhole log data (presence of a resistivity peak (dolostone bed?) and increase in potassium content in the interval above; Fig. 3). The lower limit of the hiatus is tentatively dated at >3.57 Ma: *G. punctulata* disappears between 3.57 and 3.31 Ma and this species is present in all the samples taken from below the hiatus (i.e. deeper than 462.4 mbsf). However we do not have enough samples to be sure that this short period of disappearance has not been missed. All samples close to the hiatus base analyzed in this study contained *Sphaerodinellopsis seminulina* which disappears at 3.19 Ma (Lourens, 2004) thus the base of the hiatus

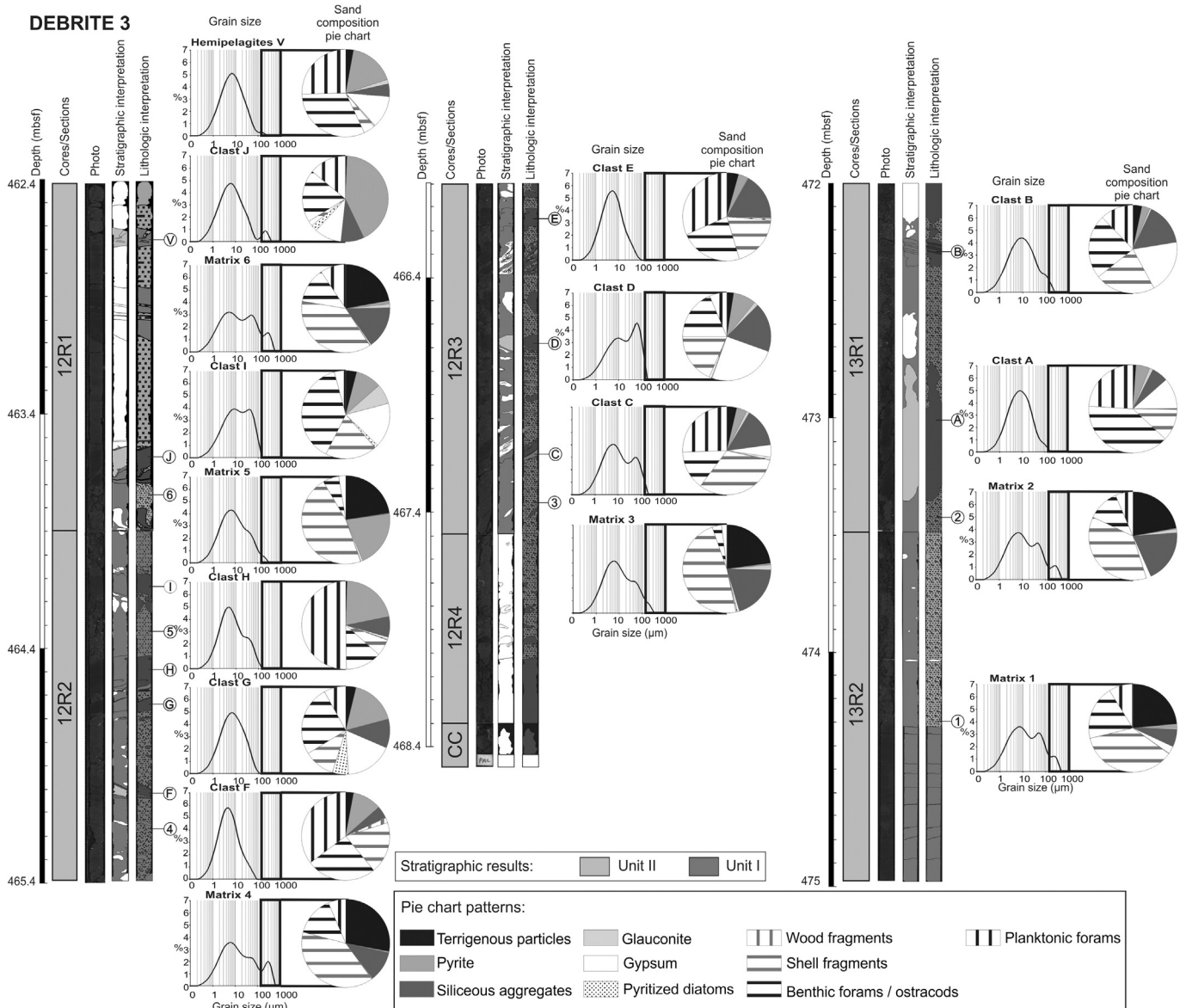


Fig. 5. Lithology and stratigraphy of the youngest and thickest debrite of the early Pliocene (D3). Sample location, grain-size results, composition of the sandy fraction and age of each sample are shown. Stratigraphic units are indicated in both cores/sections and stratigraphic interpretation boxes.

also could be placed >3.19 Ma (Fig. 2). The top of the hiatus is placed at 454.08 mbsf and has been dated at 1.66 Ma during Expedition 339 with the last occurrence of calcareous nannofossil *Calcidiscus macintyreii* (Raffi et al., 2006; Flores et al., 2010). In this study, we thus refine the duration of this hiatus to 1.65–1.91 Ma, from ~1.66 to 3.31–3.57 Ma, as it was previously estimated from ~1.66 to 3.19–3.98 Ma. Studied samples from above this hiatus have been taken from the debrites only: planktonic foraminifer *G. inflata* is present but has been reworked, and only confirm that unit III (light gray in Fig. 2; Table 1) is younger than 2.09 Ma. Age of this unit can be refined with calcareous nannofossils identified during the Expedition: the youngest age obtained for this unit at ~414 mbsf in Hole U1386C corresponds to the last occurrence of *Helicosphaera sellii* at 1.25 Ma. Unit III is thus comprised between 1.66 and 1.25 Ma (Expedition 339 Scientists, 2013).

The oldest studied debrite (D1, 497.87–496.82 mbsf; Figs. 2 and 3) belongs to unit II and deposited just above a hemipelagic deposit dated at 3.8 Ma. Samples taken above the debrite, in hemipelagic sediments, are also from unit II (3.8–3.57 Ma; Fig. 2; Table 1). This debrite is thus dated at around 3.8 Ma, assuming the absence of major erosion at its base. The second debrite (D2, 481.76–476.45 mbsf) and the thickest and third debrite (D3, 474.33–463.7 mbsf; Figs. 2 and 3; Table 1) deposited during unit II between 3.8 and 3.57 Ma. The last and youngest debrite (D4, 424.36–418.9 mbsf) deposited during unit III, between 1.66 and 1.25 Ma (Fig. 2 and Table 1). In the following sections, the three oldest debrites (Early Pliocene), emplaced before the hiatus, are named D1 to D3 and the youngest debrite (Early Pleistocene) is referred as D4.

4.2. Debrites of Pliocene age

4.2.1. Lithostratigraphy

Gravity deposits from the Early Pliocene are 64 m-thick in total and consist of 30 turbidites and 3 debrites (Fig. 2). The debrite D1 (~3.8 Ma) is 1.15 m-thick (Core U1386C-15R, Sections 4 and 5; Figs. 3 and 4). The sand content of its matrix is 13% to 18%. From grain-size curves, this matrix seems relatively homogeneous vertically through the debrite. The two sampled clasts are ~5 cm in diameter with a rounded shape and have a similar grain size with a sand content of 3–5%. The debrite D2, deposited at ~3.8–3.57 Ma is >1.6 m-thick (Core U1386C-13R, Sections 3 and 4; Figs. 3 and 4). A base of a debrite has been cored at the top of core 14. It could correspond to the base of the overlying debrite. This interpretation is supported by the downhole logs (Fig. 3). The debrite is clearly evidenced by high resistivity and density values and reflect the cemented character of the debrite. The low gamma ray content likely reflects the presence of sands and the abundance of bioclasts. The debrite extends from 477.5 to 480.9 mbsf and is 3.4 m thick. The sample collected in matrix has a sand content of 20%. Clasts are ~5 cm in diameter, except the large clast observed at the base of the debrite which is ~40 cm in diameter. Sand content of clasts ranges from 1% to 8% (Fig. 4). Sediment size fraction >150 µm has not been counted for debrites D1 and D2 as the thickness of D1 would not be representative and the missing part of D2 is larger than the recovered part.

The youngest and thickest Early Pliocene debrite D3 is observed into two cores, spanning 6 sections from Core U1386C-13R, Section 1 to Core U1386C-12R, Section 1 (Fig. 5). It is deposited above silty-clay hemipelagic sediments with planar laminations and covered by alternation of hemipelagites and turbidites. Because of similarity of matrix and clasts in Cores -12R and -13R, this debrite is considered as continuous between both cores despite a recovery problem encountered during rotary coring. The logging data support this interpretation with the presence of a highly resistive cemented interval extending continuously from Core 12R to 13R (Fig. 3). The density and gamma ray logs show a less obvious pattern because they have been affected by an enlargement of the borehole diameter over this interval. The total thickness of this debrite is 11.9 m based on core data, and 10.8 m thick (464.8–475.6 mbsf) based on downhole log analysis.

Six samples from matrix have been studied. The sand content ranges from 10% to 25%. The composition of the >150 µm fraction is characterized by a significant biogenic fraction (30–45% of bivalve, gastropod and echinoderm shell fragments and 5–30% of foraminifera and ostracods; Fig. 5). Mineral fraction is represented by terrigenous particles (mainly quartz, 20–30%) and siliceous aggregates, probably related to wet sieving (5–20%).

Observed clasts have a mean diameter of 5–10 cm with a general rounded shape. Clast A exceeds 50 cm in diameter. Planar laminations have been observed in some clasts, confirming that original material is incorporated into the flow without mixing with matrix sediment. However some clasts can also be destructured as evidenced by original planar laminations showing either micro-folds or sand injections related to matrix penetration into clast fractures. Observed clasts are vertically uniformly distributed in matrix. They have a darker color than the sediment forming the matrix, and a finer mean grain size.

Ten samples have been collected from 10 different clasts. Clasts are silty-clay and sand fraction ranges from 1% to 22%. Composition of sand (>150 µm) is mainly represented by foraminifera and ostracods (25–65%), shell fragments of bivalves, gastropods, echinoderms (3–35%), pyrite (5–35%), siliceous aggregates (5–20%) and gypsum (10–25%). Composition of >150 µm fraction of clasts is relatively homogeneous, only percentages vary (Fig. 5). State of benthic foraminifer tests does not show major differences between clasts and matrix except 2–14% of abraded tests in matrix sediment.

Composition and grain size of each clast do not allow grouping them into distinct families. Material from clast and matrix is different: clasts and matrix do not have the same origin implying that they have not been incorporated in the same time into the debris flow.

4.2.2. Origin of reworked material

Hole U1386C is presently located in the middle slope of the Algarve margin, at 565 m water depth. Benthic foraminifer and ostracod assemblages observed in samples taken in hemipelagic sediments indicate paleodepths of a bathyal environment (epibathyal to mesobathyal), ranging from 200 to >500 m (Fig. 6). Abundance of benthic foraminifers *Cibicides pseudoungerianus*, *Uvigerina proboscidea*, *U. bifurcata* and *Bulimina costata*; and ostracods *Krithe* spp. and *Henryhowella sarsi profunda* mainly indicate these paleodepths (Lutze, 1986; Van Morkhoven, 1986; Alves Martins and Ruivo Dragão Gomes, 2004; Mendes et al., 2004; Ruiz et al., 2008; Alvarez Zarikian et al., 2009). In these samples, taphonomical analysis showed presence of mainly well-preserved tests (68–85%), with some partially broken (12–25%) and pyritized tests (0.5–2%). Moreover, ostracoda show better preservation (mostly translucent valves and almost no fragmentation) in clast samples than in the surrounding matrix, where moderate to high valve fragmentation, and darkened shells are common.

Paleodepths reconstructions have been performed in detail for the thick debrite D3. Benthic foraminifera are abundant in clast and matrix samples of the thick debrite. Ostracoda are present in lower abundance. All matrix samples are dominated by shelf assemblages. Presence of benthic foraminifera such as *Asterigerinata* spp., *Cibicides lobatulus* and *Elphidium* spp.; and of ostracoda *Aurila* spp., *Burtonia* spp., *Callistocythere* spp., *Loxococoncha* spp., *Pontocythere elongata*, *Urocythereis* spp. and *Costa punctatissima* indicate infralittoral to circalittoral environments (0–100 m; Fig. 6) (Ruiz and Gonzalez-Regalado, 1996; El Mmaidid et al., 2002; Mendes et al., 2004; Ruiz et al., 2008). Equations of Van der Zwaan et al. (1990) and Wright and Berggren (1977) for benthic foraminifera are relatively well correlated, and suggest a more outer shelf environment than results from bathymetrical zonation based only on species. High abundance of planktonic foraminifera in the samples explains the deepest paleodepths given by the equations. Abundance of shell fragments of bivalves and gastropods, infralittoral ostracods, and terrigenous particles, however, confirms the shelf environment.

Paleodepth results for clast samples are less accurate than those from matrix samples. Benthic microfaunal assemblages indicate a mix

of shelf, and bathyal (upper and meso) paleoenvironments, with paleodepths ranging from 0 to 200 m for clasts A and B, from ~100 to ~300 m for clast J, from ~100 to ~500 m for clasts C, D, F and H, and from ~200 to ~500 m for clasts E and G. Clast I shows high abundance of *U. bifurcata* (44%), which is typical of water depths of 300–500 m. Clasts D, F, G, I, and J are devoid of ostracoda.

Paleodepth reconstructions indicate that the source of the clasts was slightly deeper than the sediment forming the matrix. This implies that the clasts have been integrated at a later stage during the flow. Seafloor erosion is significant in thickness (sediment from units I and II incorporated) but also in term of distance over which erosion occurred (from shelf to mesobathyal environment). Some clasts (e.g.

A, C, G or H) show mixing of benthic fauna living at different depths and inconsistency with equation results. These clasts probably come from gravity deposits that occurred before the triggering of debris flow on the slope.

The debrite D1 was deposited during unit II (3.8 - >3.57 Ma, Fig. 2). Biostratigraphical study of matrix samples however show that all the samples are dated from the same period: unit I (4.52–3.8 Ma). Sediment from matrix are thus up to 950 ka older than period of debris flow deposition. Determination of biostratigraphical units I and II being based on presence of *G. margaritae*, it is possible that during failure, sediment from both units would mixed. If that is the case, only the oldest unit is evidenced. Biostratigraphical analysis of clasts indicates that clasts

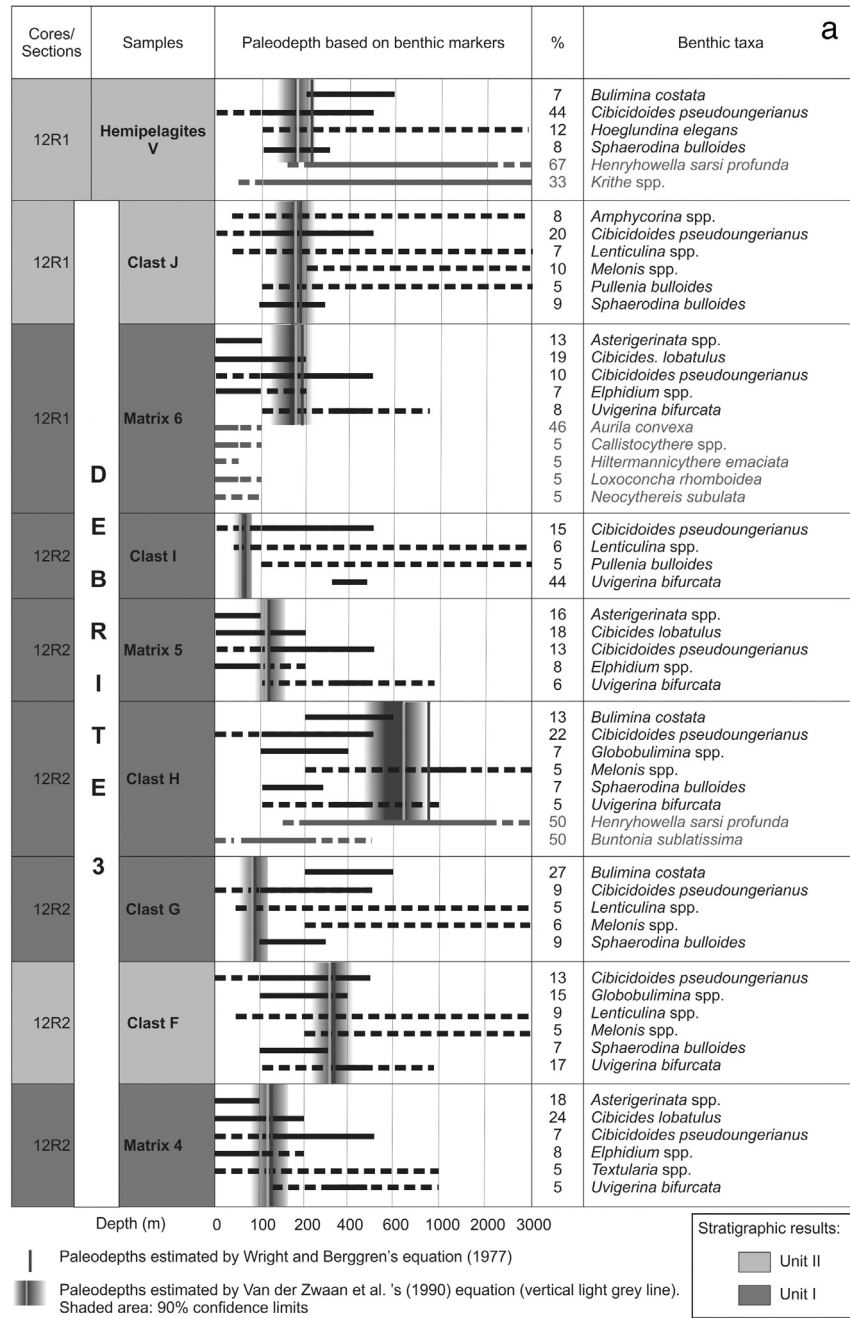


Fig. 6. (a): Bathymetric estimation from benthic foraminifers (black) and ostracods (dark gray), and results from equations of Van der Zwaan et al. (1990) and Wright and Berggren (1977) in samples from the thickest debrite of the Early Pliocene (D3). Stratigraphic units are indicated in cores/sections and sample boxes. (b): Following the results of debrite 3. * corresponds to paleodepths inferred based on species from the same genus.

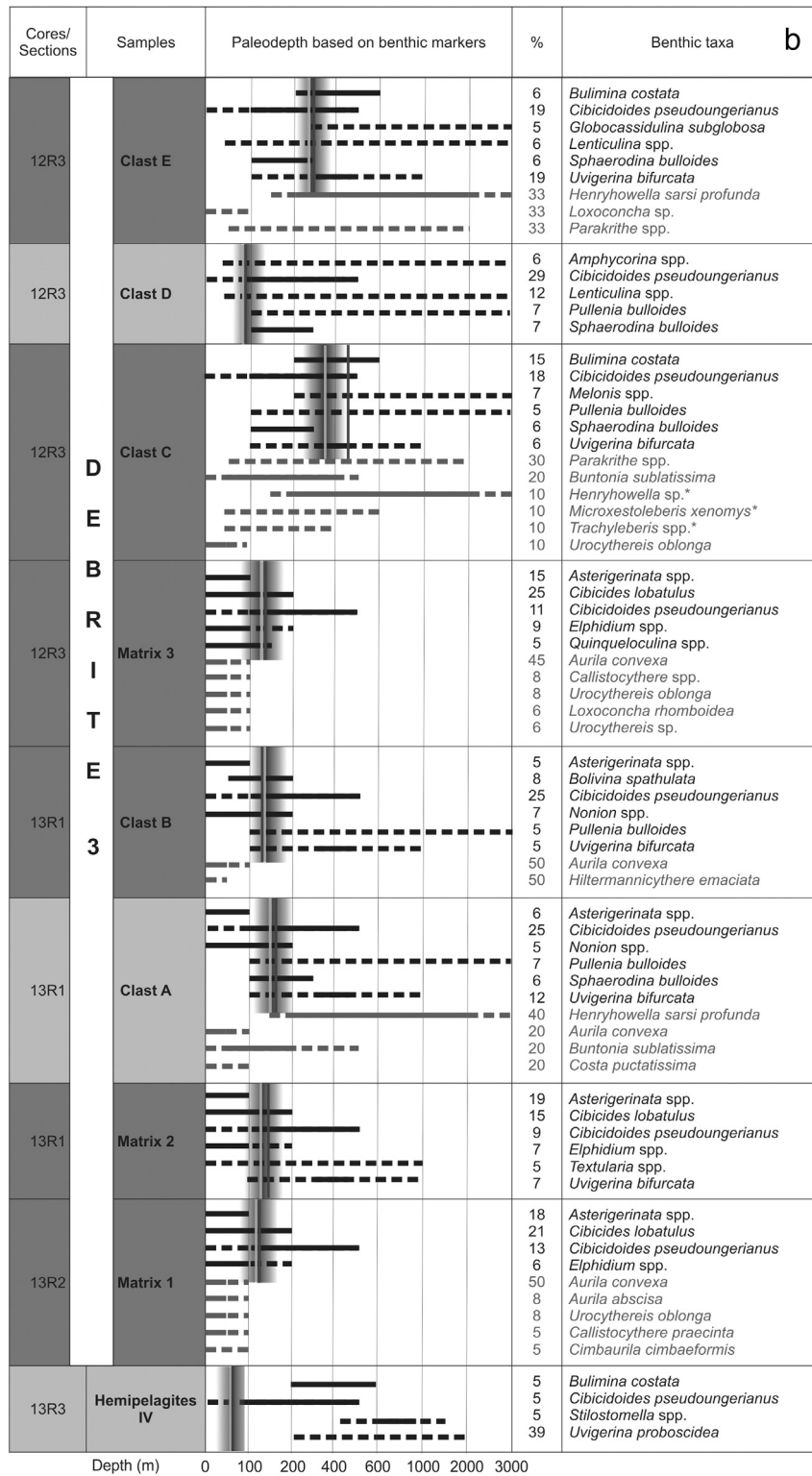


Fig. 6 (continued).

belong to units: I (clasts B, C, E, G, H and I) and II (clasts A, D, F and J). Clasts are not organized according to their age or source paleo-depth inside matrix and there is no clear evidence of relationship between age and related depth in clasts (Fig. 6).

In the debrite D1, reworked sediment is either older or of the same age than debrite initiation. This debris flow displaced sediment older and coeval of deposition area. These reworked sediments belonged to ancient turbidites and hemipelagites. Erosion of the sea floor (failed

sediment and sediment eroded along the flow pathway) during this debris flow has been significant.

4.3. Debrite of early Pleistocene

4.3.1. Lithostratigraphy

Total thickness of gravity deposits from early Pleistocene is ~50 m with about 30 turbidites and one debrite. This debrite D4 is observed

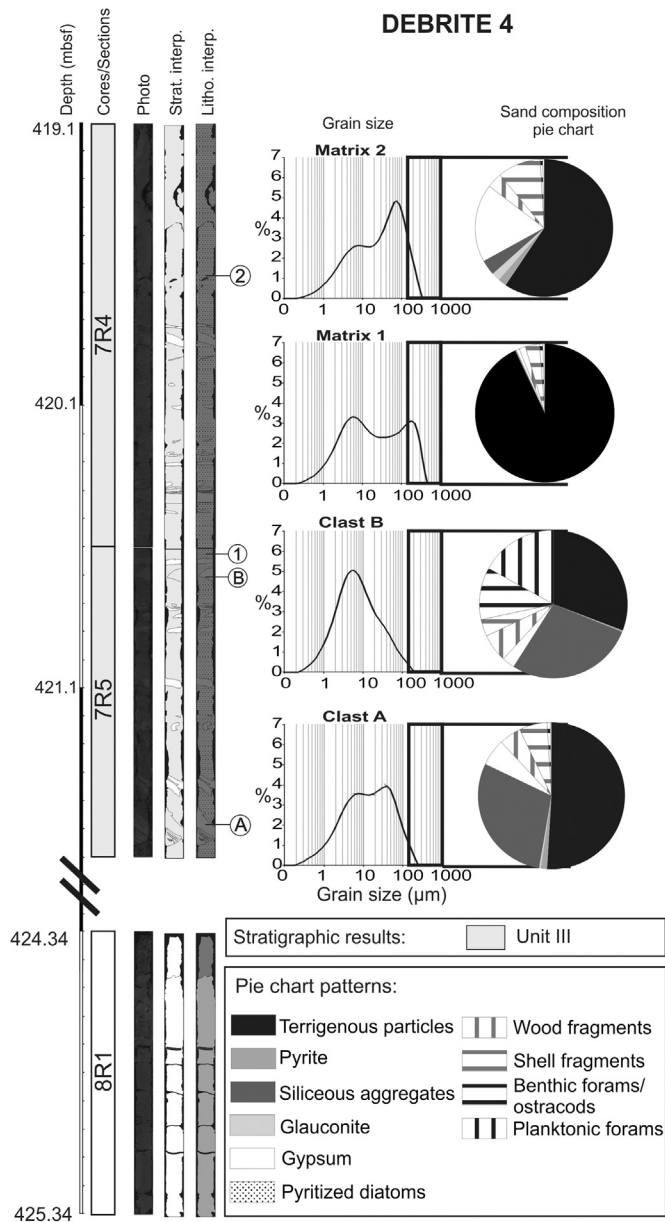


Fig. 7. Lithology and stratigraphy of gravity deposits from the early Pleistocene. Sample location, grain-size results and composition of the sandy fraction of each sample of the debrite D4. The stratigraphic unit is indicated in both cores/sections and stratigraphic interpretation boxes.

in two cores and three sections (U1386C-8R-1 to 7R-4; Fig. 7). It is deposited between carbonate silty-clay sediment at its base and several turbidites with the same lithological composition than the debrite at the top. Despite that there is no sample in Core 8R, this debrite is considered as continuous between both cores based on wireline logging data, and comparison of the log patterns with the ones of the petrophysical core logs (Fig. 3). This debrite is 5.40 m thick based on core data, and 6.9 m thick based on donwhole logs (418.5–425.4 mbsf).

Only four samples have been studied in debrite D4 (as clasts were few in number and most of them small in size): 2 clasts (A and B) and 2 matrix (1 and 2) samples. Samples from matrix are characterized by 32 and 34% of sand. Composition of the sediment fraction >150 µm shows a very important terrigenous fraction: 70–95%, mainly represented by lithic fragments (quartzite with quartz with wavy extinction), quartz, plagioclase feldspars and micas. Biogenic fraction is mainly

composed of shell fragments from bivalves, gastropods and echinoderms (2 and 10%) and a small amount of foraminifera and ostracoda. Gypsum is observed (15%) in one sample (Matrix 2; Fig. 7). State of foraminifer tests shows black tests (5%) and 7–11% of broken tests. The high terrigenous content in this debrite is supported by magnetic susceptibility values much higher than in the Early Pliocene bioclast-rich debrites (Fig. 3), biogenic components being diamagnetic. The gamma ray signal is also higher in the Early Pleistocene debrite D4, likely reflecting enrichment in potassium content (Fig. 3) due to the presence of plagioclase feldspars in the matrix.

Clast A is around 8 cm in diameter. It is composed of 15% of sand and shows planar laminations and matrix injections. Fraction >150 µm is characterized by 50% of terrigenous particles (mainly micas, quartz and lithic fragments similar to those of matrix), 35% of siliceous aggregates (probably newly formed), 5% of wood fragments, 5% of shell fragments, and 5% of gypsum. Clast B is around 3 cm in diameter with a rounded and elongated shape. Its sand content is only 6%, composed of 30% of terrigenous particles (micas, quartz and lithic fragments), 30% of siliceous aggregates, 25% of foraminifera and ostracods, and 5% of wood fragments. State of tests shows ~5% of broken tests in both clasts, and 19% of black tests in clast A.

Composition and grain size are relatively different in the two clasts, indicating a different origin. Clasts and matrix are not composed of the same sediment suggesting that the clasts have been integrated into the matrix during the debris flow.

4.3.2. Origin of reworked material

Benthic foraminifer and ostracod assemblages from matrix samples show relatively similar paleodepths related to shelf environment (0–200 m). Foraminifera *C. carinata*, *C. lobatulus*, *Elphidium spp.* and *Quinqueloculina spp.* and ostracoda *Aurila spp.*, *Callistocythere spp.*, *Palmoconcha turbida*, *Pontocythere elongata* and *Sagmatocythere multiforma* are typical from this shallow environment (El Mmaïdi et al., 2002; Ruiz et al., 2008; Fig. 8). Equations from Van der Zwaan et al. (1990) and Wright and Berggren (1977) fit with data from foraminifer species assemblages and give paleodepths ranging from 100 to 200 m. High proportion of terrigenous particles in samples and presence of bivalve and gastropod fragments confirm this shallow deposition environment of material forming the matrix before failure.

Clast samples show different paleodepths: clast A seems to originate from a shelf and inner shelf environment as indicated by the presence of benthic foraminifera *C. carinata*, *Elphidium spp.*, *N. turgida*, *B. marginata* and *B. gibba*, and ostracoda *Aurila convexa*, *Loxoconcha rhomboidea*, *Callistocythere spp.*, *Leptocythere sp.*, *Neocythereis subulata*, etc. This sample shows moderate fragmentation of ostracod valves. In contrast, microfungal assemblages in clast B indicate that it originated from an area located between inner/outer shelf and epibathyal domain (abundance of *C. pseudoungerianus*, *N. turgida*, *S. bulloides* and *C. carinata*; and the presence of the inner-shelf ostracoda *Loxoconcha spp.*, *Aurila spp.*, and *Urocythereis spp.* and deeper water *Krithe spp.*, *Cytheropteron sp.*, *Argilloecia sp.*, and *Pseudocythere caudata*; Fig. 8). Such as the matrix sediment, clast A seems to come from an area located close to the failure area, while clast B has been integrated to the flow later and at a deeper depth. Clast B shows a mixing of benthic fauna that could suggest that the material composing the clast consisted of sediment previously reworked along slope (nepheloid or low density turbidity current). Presence of wood fragments in all samples testifies that downslope transfer occurred rapidly from continental domain to marine gravity deposits.

Biostratigraphical analysis indicates that all sediments forming the debrite are younger than 2.09 Ma and belong to unit III. Analysis of calcareous nannofossils allowed refining ages between 1.66 and 1.25 Ma. The debrite probably emplaced closer to 1.25 Ma (Fig. 2). It was not possible to find hemipelagic sediment just above or below the gravity deposits in order to refine the age of this debrite.

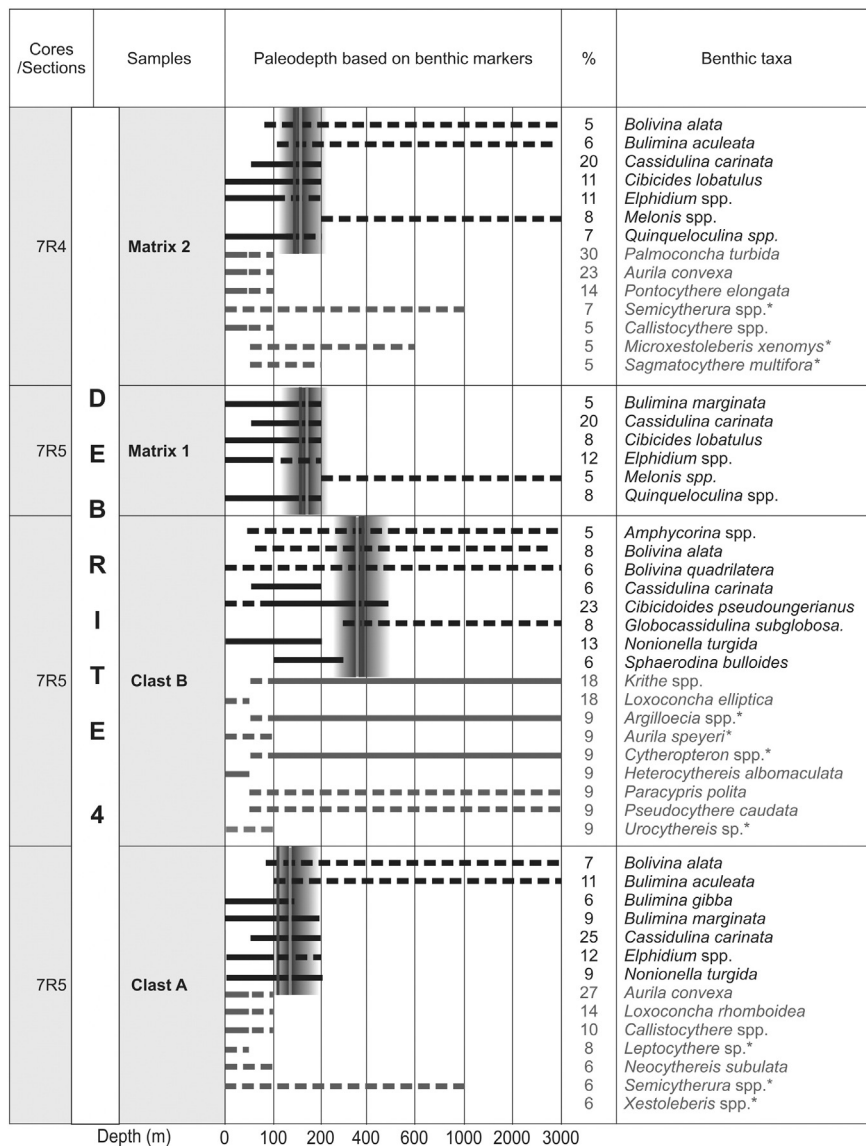


Fig. 8. Bathymetric estimation from benthic foraminifers (black) and ostracods (dark gray), and results from equations of Van der Zwaan et al. (1990) and Wright and Berggren (1977) in samples from debris of the early Pleistocene (D4). * corresponds to paleodepths inferred based on species from the same genus. The stratigraphic unit is indicated in cores/sections and sample boxes.

Discussion

4.4. Estimation of erosive behavior of debris flows

4.4.1. Debrites from the early Pliocene

Debrites from the Early Pliocene have clasts with finer grain size than matrix. They are regularly distributed in matrix, without any particular organization related to age of sediment or paleodepth. In the debrite D3, the matrix and the clasts A and B (Fig. 9) have the same range of origin, in term of paleodepths, and are all originated from the shelf. The grain-size and composition of sediment size fraction >150 µm are however very different implying a difference in the sediment source. This suggests that over the Early Pliocene, the substratum of the shelf of the Algarve margin was heterogeneous, as it is the case now close to Guadiana mouth (Mendes et al., 2012). The other clasts have been eroded during the flow from the outer shelf down to the deposition area (from 100 to 500 m water depth; Fig. 9). A large part of the Guadalquivir basin was flooded but the morphology of the Algarve margin is not accurately known for the early Pliocene, it has been considered that it was relatively similar to the present

(Hernández-Molina et al., 2006; Fig. 9). Assuming that the shelf and upper slope had approximately the same width than today, the debris flows would have a run-out distance of less than 100 km, eroding material of the same age as well as underlying deposits (units I and II; Fig. 9). The difference of thickness between the three debrites of Early Pliocene could be explained by different failure volumes and/or a more or less erosive behavior.

Roque et al. (2012) do not evidence turbiditic channels in the area during the Early Pliocene suggesting that debris flows would have run on the open slope. However, without strike (East–West) seismic lines on the shelf, it is difficult to confirm that those debrites were not channelized. Brackenridge et al. (2013) and Martínez del Olmo (2004) suggest some preferential pathways sourcing from the northeast without describing permanent channels (Fig. 9). Regardless the channelization degree of these debris flows, the high difference of composition between matrix and some clast samples sourcing from the shelf and other clasts originating from epi- to mesobathyal environments indicates an erosive behavior along the pathways of these debris flows.

In the eastern part of the Gulf of Cádiz, unit D (5.3–2.5 Ma) described by Ledesma (2000), is 500–600 m-thick and corresponds to hemipelagic

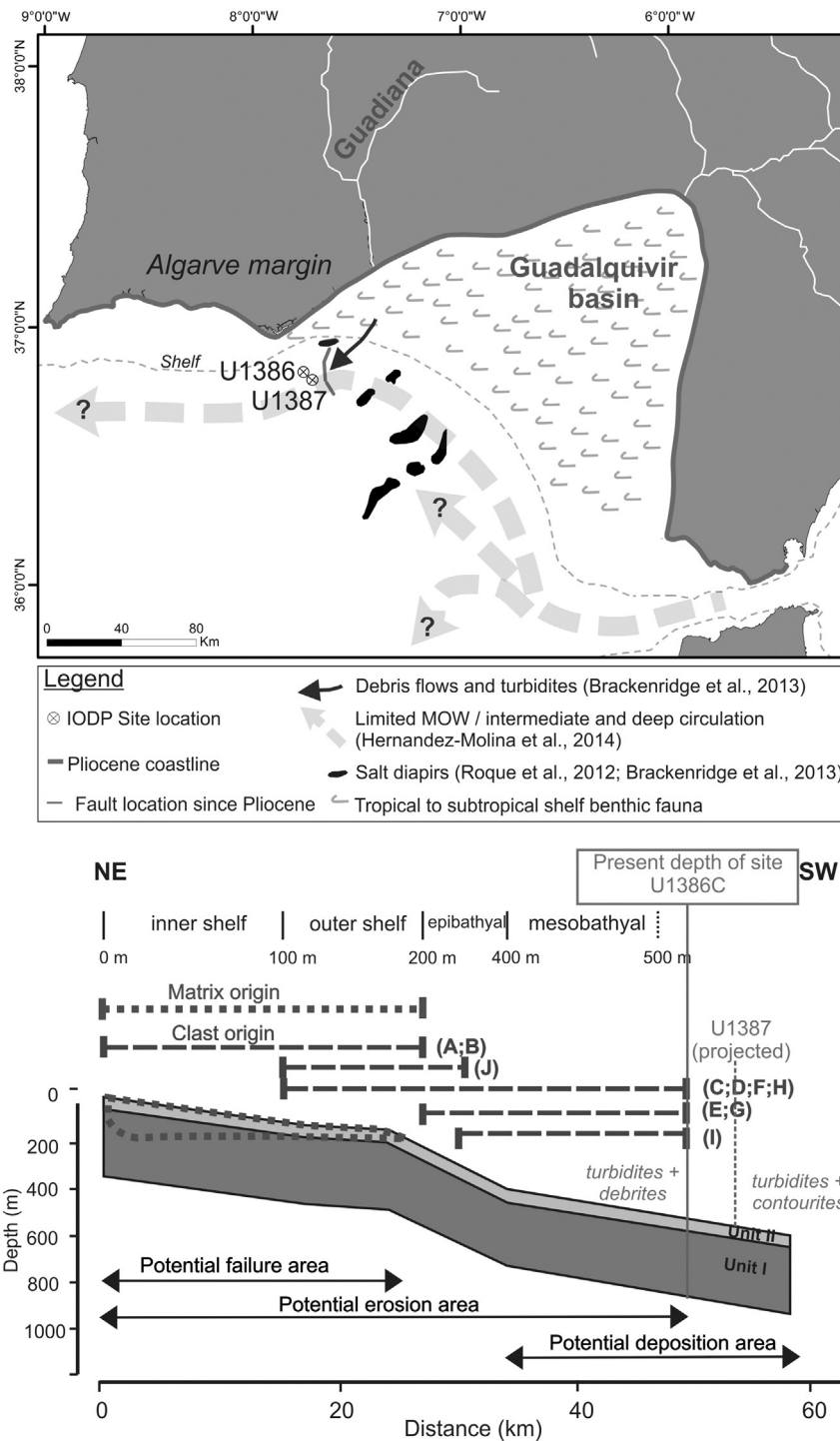


Fig. 9. Synthesis of the origin of clasts and matrix from early Pliocene debris D3.

deposits (F.J. Siero, pers. Comm.). The sedimentation rate in this unit approximates 200 m/Ma. The presence of a hiatus within this time interval (5.3–2.5 Ma) indicates that this estimation is very rough but may be useful to estimate the amount of material reworked/eroded into/by the debris. Using this mean sedimentation rate, the expected thickness of combined units I and II (5.34 and 3.57 Ma) at the studied location should be ~350 m. On shelf and upper slope, this thickness is expected to be reduced because of the geometry of the margin consisting of prograding wedges. In any case, depositional units associated to units I and II are not of the order of meters or decimeters thick but a hundred meters thick indicating that the failure areas were probably important in size.

As thicknesses of debris are only decimeter scale, it can be suggested that the failed sediment volume has been deposited through wide but thin debris flows or only a part of these failed sediments has been transformed from gliding to flow process. In this example, matrix is typically composed of failed sediments whereas clasts are either coming from the failed area or from the erosion along the flow pathway.

4.4.2. Debrite from the early Pleistocene

Clasts of the debris D4 are regularly distributed in the matrix. Silty-clay hemipelagic sediment under the debris is dated around 1.61 Ma and sediment overlying the debris are ~1.25 Ma. Sediment displaced

by the debris flow is dated at 1.25 Ma suggesting that ~350 ka of sediment deposition are missing. These missing sediments could have been eroded before or during the debris flow or not have been deposited because of an intense MOW activity.

Clast B has a higher foraminiferal content and different microfaunal composition (benthic foraminifera and ostracoda) than clast A, and their original paleodepth is different (Fig. 10). Eroded volume during the flow is difficult to estimate because the thickness of the early Pleistocene hemipelagic deposits is unknown. This debris flow was probably triggered on the inner or outer shelf and clasts indicate that the flow eroded the slope at least down to ~400 m of water depth. The debris flow probably did not erode all along its pathway because of the lack of mesobathyal species observed. Interpretations of flow

erosion, especially for two clasts showing different information, are however not fully relevant in a statistic point of view, and they have to be considered with caution. The run-out distance of this debris D4 is similar to the run-out distance of the debris D3 dated from the Early Pliocene.

4.5. Potential pre-conditioning factors to flow triggering

4.5.1. Sediment sources and shelf storage

Early Pliocene and Early Pleistocene debris show a similar pattern. The matrixes and some of the clasts originated from the shelf environment while some other clasts came from the upper slope. These debris are also embedded with turbidites and are not isolated in hemipelagic

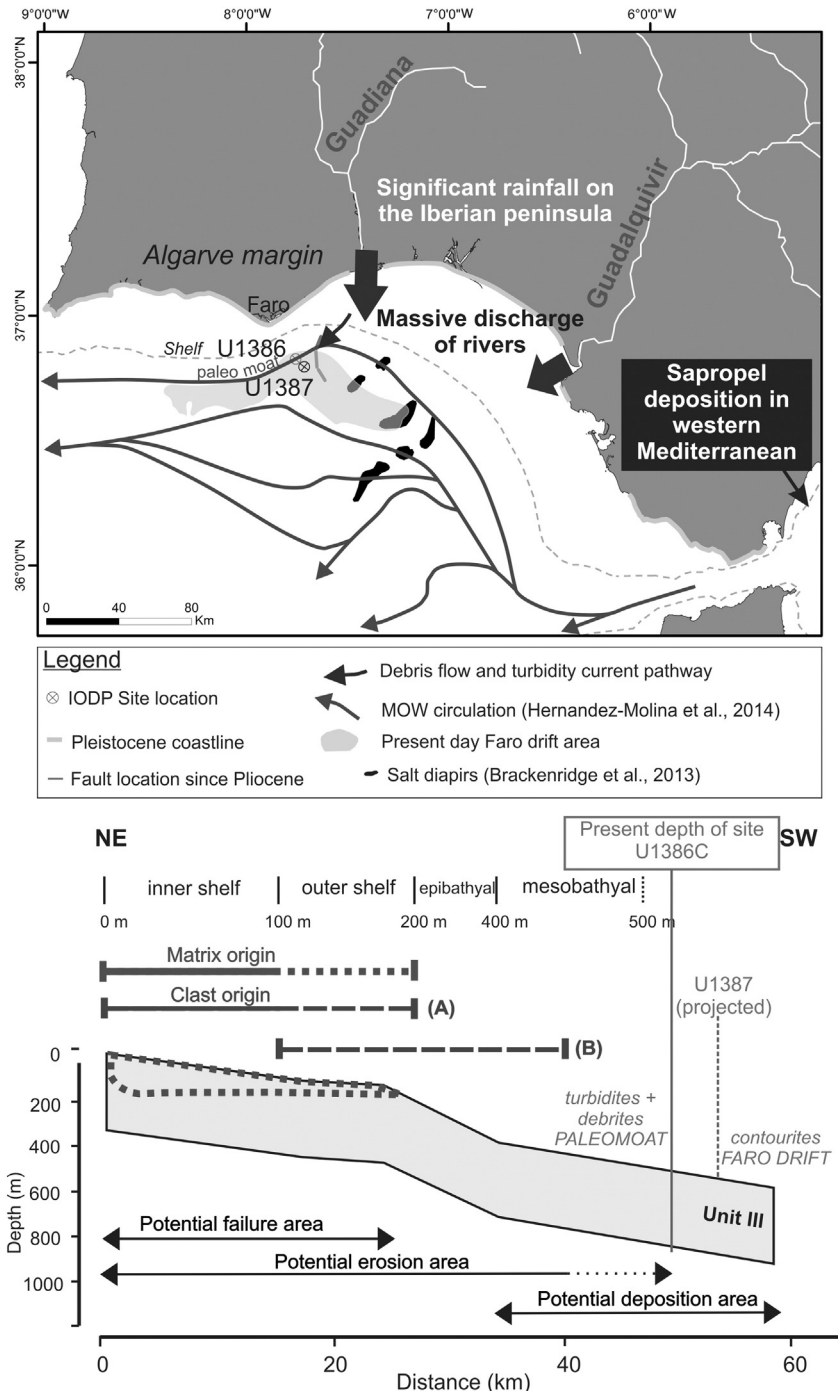


Fig. 10. Synthesis of the origin of clasts and matrix from early Pleistocene debris D4.

sequences. However, they are different in age and sediment composition (Figs. 9 and 10). Early Pliocene debrites D1 to D3 have a greater proportion of biogenic particles (Fig. 5), whereas the early Pleistocene debrite D4 has a greater terrigenous content (Fig. 7). During the Pliocene, continental supplies in the Gulf of Cádiz were coming from two main rivers which drained the south of Spain: the Guadalquivir River (East) and the Guadiana River (North; Ledesma, 2000; Fig. 1).

Biogeographical models of the eastern part of the Gulf of Cádiz showed a significant change between the Pliocene and the Pleistocene: Monegatti and Raffi (2007) and Marques da Silva et al. (2010) describe a high concentration of fossils during the Early Pliocene on continental shelves. This high concentration is explained by a warm climate and a relative high and stable global sea level (Miller et al., 2005) allowing the development of abundant tropical to subtropical shelf species (Fig. 9). This is in accordance with the abundance of bivalve, gastropod, echinoderm, and ostracod fragments observed in the Early Pliocene gravity deposits. Between the Pliocene and the Pleistocene, temperate and tropical fronts migrated southward of Iberia peninsula, leading to a cooling and a decrease of biodiversity in the area (Monegatti and Raffi, 2007; Marques da Silva et al., 2010). This cooling is suggested by the first appearance of typical deep, cold-water ostracods *Pseudocythere caudata mediterranea* and *Cytheropteron* spp., and could explain the weaker proportion of shelf fossil fragments into the early Pleistocene debrite and turbidites.

The Guadalquivir and Guadiana rivers, the main terrigenous sources of the Gulf of Cádiz over Plio-Pleistocene, have very close drainage basins and drained geological units are relatively similar. The Guadalquivir basin drains mainly the Betic ranges and extended geological units (Iribarren et al., 2009) whereas the Guadiana basin crosses a great number of various small geological units (Gabaldon, 1994). The Guadiana River passes through slightly more metamorphic and plutonic provinces than the Guadalquivir River. High abundance of feldspars, quartz and quartzite with quartz with wavy extinction in samples from gravity deposits implies an important metamorphic origin and could preferentially come from the Guadiana River. The vicinity between Guadiana mouth and gravity deposit area could indicate also that terrigenous sand fraction could preferentially come from the Guadiana River, especially during early Pleistocene (Fig. 10).

The seismic reflection line P74–45 shown by Hernández-Molina et al. (2014) illustrates the different depositional architectures of the Algarve margin at the location of Sites U1386 and U1387. Depositional units I and II, characterized by turbidites and debrites at Site U1386, show thicker deposits at Site U1387 (4 km southward) with the first contourites interbedded with turbidites and forming a sheeted drift (phases 1 and 2 in Hernández-Molina et al., 2014, corresponding to the onset of limited MOW circulation with intermediate to deep pathways; Fig. 9). The hiatus of the late Pliocene and the base of the Quaternary correspond to a regional discontinuity related to enhanced MOW circulation and erosion by bottom currents (phase 3 in Hernández-Molina et al., 2014). At other Expedition 339 sites, the hiatus observed in late Pliocene is characterized by a dolostone bed (Expedition 339 Scientists, 2013; Hernández-Molina et al., 2013, 2014). Depositional unit III is very different at Sites U1386 and U1387 with turbidites, a debrite and erosion related to moat formation at Site U1386, and contourites southward at Site U1387 (phase 4 in Hernández-Molina et al., 2014, with the establishment of present-day circulation of MOW). The moat formation along the Algarve margin related to MOW intensification created a trough that could have channelized turbidity currents and debrites coming from the north and northeast margin, preventing their deposition southward (Fig. 10). Upslope migration of this moat and the Faro associated drift during Pleistocene explains the lack of gravity deposits observed at Site U1386 after 1.25 Ma. This transition from a Pliocene mixed system with interacting down-slope and along-slope processes to a Quaternary contourite-dominated margin is also well described in the seismic synthesis from Brackenridge et al. (2013).

4.5.2. Environmental conditions and tectonic activity

During the Early Pliocene and the period of gravity flows enriched in bioclastic fragments, Mediterranean climate was warmer and wetter than present (Lourens et al., 1996) and relative sea level was high and stable (Miller et al., 2005). Cooling periods have been identified: the first one at 3.7 Ma, the second one between 3.5 and 3.2 Ma (Lourens et al., 1996). Temperatures decreased during these periods but moisture was still high. In the Gulf of Cádiz, activity periods of MOW punctuated the Pliocene deposits with one period of intensification between 3.5 and 3 Ma (Khélifi et al., 2009; Brackenridge et al., 2013) and another one between 2.4 and 2.1 Ma (Zitellini et al., 2009; Brackenridge et al., 2013). Thus the ~2 Ma long hiatus (<3.57–1.66 Ma) observed above the Early Pliocene thick debrite may be related to these periods of MOW intensification. On the other hand, the studied gravity deposits are particularly thick and sedimentation observed between the debrites is hemipelagic, with no evidence for contourite deposits at Site U1386. These hemipelagites are characterized by centimeter to millimeter-scale laminae and absence of bioturbation, suggesting absence of current during sedimentation. The Early Pliocene gravity deposits in the area may thus have emplaced when MOW was flowing at deeper water depth than the one at the drilling site as it is suggested from seismic data by Hernández-Molina et al. (2014); Fig. 9).

The start of glaciations in the northern hemisphere is documented around 2.7 Ma. Growth and progress of ice southward initiated colder and drier conditions in Mediterranean and northern Atlantic areas, reducing intensity of ocean circulation through Atlantic and favoring MOW establishment (Hernández-Molina et al., 2014). Early Pleistocene debris flows and turbidity currents flowed around 1.25 Ma. Paleo-moat location at site U1386 during this period explains the condensate sedimentation associated to coarse sediment and gravity deposits (Fig. 10). However, between 1.66 and 1.25 Ma (unit III), 7 sapropels have been described in the Alboran Sea and in eastern Mediterranean (Murat, 1999). Sierro et al. (2000) and Ledesma (2000) showed that logging data (gamma ray and sonic) from industrial drill sites in the Gulf of Cádiz fit with Milankovitch astronomical cycles (excentricity, precession and insolation) and with biostratigraphy established at Cap Rossello (Sicily, Lourens et al., 1996; Sierro et al., 2000). Peaks of gamma ray (or sonic speed) correspond to maxima of insolation and minima of excentricity (400 ka cycles) and of precession (20 ka). These astronomical periods are related to rainfall maxima over Iberia and Mediterranean Sea, and gray marl deposition during early Pliocene and sapropels from upper Pliocene (Sierro et al., 2000). Recurrence of wet events is significant during this period with high rainfall over the Mediterranean Sea and Iberia. This could be the parameter favoring riverine input into the Gulf of Cádiz and deposition of very terrigenous units, potentially reworked in gravity deposits at a later stage (Fig. 10). Brackenridge et al. (2013) did not identify however any gravity deposits in their seismic lines and they described the early Pleistocene as a period dominated by contouritic processes on the Algarve margin. Contourite deposits are well developed in Site U1387 (4 km southward; Expedition 339 Scientists, 2013) but are almost absent from Site U1386 between 1.66 and 1.25 Ma (unit III). Gravity deposits observed in Site U1386 between 1.66 and 1.25 Ma represent ~50 m in thickness and could be difficult to identify in seismic lines and could be localized along the margin. These gravity deposits that could have been channelized by the paleo-moat, also did not show a clear influence of a bottom current flowing at the same time such as a winnowing of fine particles. Sands are not clean and wood fragments are observed in debrite as in turbidite deposits. These clues could suggest either high riverine input dominating temporarily the MOW influence or a phase of weaker MOW at Site U1386 location between 1.66 and 1.25 Ma after an intense erosional phase from <3.57 to 1.66 Ma (hiatus in Site U1386) related to MOW intensification and moat emplacement. The MOW core could have move temporarily to a deeper location during this interval, related to dryer phases as described by Rogerson et al. (2005).

The high biodiversity on shelves during the Early Pliocene and the high terrigenous inputs during the Early Pleistocene resulted in significant sedimentation on the shelves. These deposits could have been easily reworked during or afterward these periods, coupled with different triggering parameters such as sea-level fall, and diapiric or seismic activity. Roque et al. (2012) and Brackenridge et al. (2013) described an intense diapiric activity during the Early Pliocene on the Algarve margin which could also be a triggering parameter of gravity flows. Presently this margin also sustains numerous earthquakes. The main seismogenic area is localized in the Guadalquivir Bank area (e.g. Borges et al., 2001), just southward of the gravity deposit area studied in this work. Most of faults of south Iberia extend into the Gulf of Cádiz, such as Sao Marcos Quarteira fault (SMQF) oriented NW-SE and extended on the continental shelf, south of Faro (Noiva et al., 2010). This fault starts to be active from the Early Pliocene (Noiva et al., 2010; Roque et al., 2012), and could be another triggering parameter of gravity deposits. Presence of wood fragments in sediment from the Early Pleistocene debrites and turbidites is in favor of a short storage of sediment on continental shelf before flow triggering.

5. Conclusions

Since the opening of the Gibraltar strait at the end of the Messinian, a large part of the present day morphology of the margins in the Gulf of Cádiz is related to MOW circulation which led to contourite deposits and drift growth. Over the Plio-Quaternary, at least two periods have however been characterized by significant and dominating gravity deposits on the Algarve margin.

Debrites and turbidites have been observed at Site U1386 (Expedition IODP 339, Hernández-Molina et al., 2013) on the Algarve margin. These gravity deposits occurred during the Early Pliocene (3.8–3.57 Ma) and the early Pleistocene (~1.25 Ma) and are relatively thick (45 and 10 m, respectively). Debrites and turbidites from the Early Pliocene are characterized by a sand fraction enriched in bioclastic fragments with silty-clay clasts in debrites, whereas gravity deposits from the early Pleistocene have a terrigenous sand fraction and silty-clay clasts in debrite. Benthic foraminifer and ostracod assemblages and percentages of planktonic foraminifera gave estimations of origin of reworked material into debrites, importance of flow erosion and run-out distances. Equations used to determine paleodepths can underestimate depths because of possible enrichment in planktonic foraminifera of sediment. Benthic foraminifer and ostracod assemblages are most of the time more valuable and give ranges of paleodepths relatively reliable despite their lack of accuracy, benthic foraminifera being widely distributed depending of species.

Debris flows from the Early Pliocene studied in this work have been erosive over their entire pathway (less than 100 km) between failure and deposition area whereas the debris flow from the early Pleistocene seems to be erosive only during the first part of its pathway. Matrixes from the two kinds of debrites initiated from the continental shelf and clasts have been incorporated from shelf to mesobathyal depths. Eroded sediments along the flow pathway seem to be integrated into the flow as clasts whereas sediments from the failure area are typically preserved in the flow matrix. Difference between both kinds of debrites and turbidites (bioclastic rich vs terrigenous rich) can be explained by different climates and relative sea levels, and more or less terrigenous input. The Early Pliocene in the Gulf of Cádiz is characterized by a warm tropical to subtropical climate and a great biodiversity of benthic fauna on continental shelves, recorded in sand fraction of gravity deposits. The early Pleistocene is marked by a colder and wetter climate with significant riverine input associated to the contouritic paleo-moat location at the studied site. This paleo-moat has favored gravity processes along the Algarve margin through this channeling feature in a close interaction between MOW circulation and down-slope processes. Triggering parameters of those gravity flows on shelf could be related

to high sediment accumulation or input during both periods, coupled with sea level falls, intense tectonic and/or diapiric activity in the area.

These two periods with significant gravity deposits on the Algarve margin are also probably related to a weak or deeper activity of MOW and are coeval with the beginning of Faro contouritic drift formation.

Acknowledgments

The INSU post-campagne program and Action Marges (INSU) are thanked for financial support. We thank the IODP core repository at Bremen, Germany, for their assistance during debrite sampling. This paper relies on the MSc2 project of Léa Fournier (Université de Bordeaux). This research used samples and data provided by the Integrated Ocean Drilling Program and collected during IODP Expedition 339.

References

- Alvarez Zarkian, C.A., Stepanova, A.Y., Grütznier, J., 2009. Glacial-interglacial variability in deep-sea ostracod assemblage composition at IODP site U1314 in the subpolar north Atlantic. *Mar. Geol.* 258, 69–87. <http://dx.doi.org/10.1016/j.margeo.2008.11.009>.
- Alves Martins, M.V., Ruivo Dragao Gomes, V.d.C., 2004. Foraminíferos da Margem Continental NW Ibérica: Sistemática, Ecologia e Distribuição. *Agenda Comum - Comunicação Lda* (367 pp.).
- Bonaduce, G., Ciampo, G., Masoli, M., 1975. Distribution of Ostracoda in the Adriatic Sea. *Publicazioni della Stazione Zoologica di Napoli* 40, pp. 1–304.
- Boomer, I., Horne, D.J., Slipper, I.J., 2003. The use of Ostracodes in Paleoenvironmental Studies, or What can you do with an Ostracode Shell? In: Park, L.E., Smith, A.J. (Eds.), *Bridging the gap. Trends in the Ostracode Biological and Geological Sciences. The Paleontological Society Papers* 9, pp. 153–180.
- Borges, J.F., Fitas, A.J.S., Bezzeghoud, M., Teves-Costa, P., 2001. Seismotectonics of Portugal and its adjacent Atlantic area. *Tectonophysics* 337, 373–387.
- Brackenridge, R.E., Hernandez-Molina, F.J., Stow, D.A.V., Llave, E., 2013. A Pliocene mixed contourite-turbidite system offshore the Algarve margin, gulf of Cadiz: seismic response, margin evolution and reservoir implications. *Mar. Pet. Geol.* 46, 36–50.
- Carter, L., 2001. A large submarine debris flow in the path of the Pacific deep western boundary current off New Zealand. *Geo-Mar. Lett.* 21, 42–50.
- Cimerman, F., Langer, M.R., 1991. *Mediterranean Foraminifera*. Slovenska Akademija, Ljubljana (93 pp.).
- Dayja, D., 2002. *Les Foraminifères Néogènes, Témoins de la Chronologie, de la Bathymétrie, et de l'Hydrologie du Corridor Rifain (Maroc Septentrional)* PhD thesis, Université Pierre et Marie Curie, Paris (unpublished).
- De Rijk, S., Troelstra, S.R., Rohling, E.J., 1999. Benthic foraminiferal distribution in the Mediterranean sea. *J. Foraminif. Res.* 29, 93–103.
- Ducassou, E., Migeon, S., Capotondi, L., Masclé, J., 2013. Run-out distance and erosion of debris-flows in the Nile deep-sea fan system: evidence from lithofacies and micropaleontological analyses. *Mar. Pet. Geol.* 39, 102–123.
- El Mmaid, A., El Mounni, B., Nachite, D., Gensous, B., Monaco, A., 2002. Distribution et Caractères de la Microfaune d'Ostracodes Dans les Dépôts Superficiels de la Partie Occidentale de la Marge Méditerranéenne Marocaine. *Bulletin de l'Institut Scientifique, Rabat, section Sciences de la Terre* 24, pp. 15–22.
- Expedition 339 Scientists, 2013. Site U1386. In: Stow, D.A.V., Hernández-Molina, F.J., Alvarez Zarkian, C.A., and the Expedition 339 Scientists, Proc. IODP, 339: Tokyo (Integrated Ocean Drilling Program Management International, Inc.). doi:<http://dx.doi.org/10.2204/iodp.proc.339.104.2013>
- Faranda, C., Gliozzi, E., 2008. The ostracod fauna of the plio-pleistocene Monte Mario succession (Roma, Italy). *Boll. Soc. Paleontol. Ital.* 47 (3), 215–267.
- Fariduddin, M., Loubère, P., 1997. The surface ocean productivity response of deeper water benthic foraminifera in the Atlantic ocean. *Mar. Micropaleontol.* 32, 289–310.
- Faugères, J.-C., Cremer, M., Monteiro, H., Gaspar, L., 1985. *Essai de reconstitution des processus d'édification de la ride sédimentaire de Faro (marge Sud-portugaise)*. Bull. Inst. Géol. Bassin Aquitaine 37, 229–258.
- Flores, J.-A., Colmenero-Hidalgo, E., Mejía-Molina, A.E., Baumann, K.-H., Henderiks, J., Larsson, K., Prabhu, C.N., Sierro, F.J., Rodrigues, T., 2010. Distribution of large *Emiliania huxleyi* in the central and northeast Atlantic as a tracer of surface ocean dynamics during the last 25,000 years. *Mar. Micropaleontol.* 76, 53–66.
- Gabaldon, V., 1994. Mapa geológico de la península ibérica, Baleares y Canarias, escala 1 : 1 000 000. Instituto tecnológico geominero de Espana con la colaboración del instituto geológico e mineiro de Portugal.
- Gonthier, E.G., Faugères, J.-C., Stow, D.A.V., 1984. Contourite facies of the Faro drift, gulf of Cadiz. *Geol. Soc. Lond. Spec. Publ.* 15, 275–292.
- Haughton, P.D.W., Barker, S.P., McCaffrey, W.D., 2003. 'Linked' debrites in sand-rich turbidite systems - origin and significance. *Sedimentology* 50, 459–482.
- Hernández-Molina, F.J., Llave, E., Stow, D.A.V., García, M., Somoza, L., Vázquez, J.T., Lobo, F.J., Maestro, A., Diaz del Río, V., León, R., Medialdea, T., Gardner, J., 2006. The contourite depositional system of the Gulf of Cadiz: a sedimentary model related to the bottom current activity of the Mediterranean outflow water and its interaction with the continental margin. *Deep-Sea Res.* II 53, 1420–1463.
- Hernández-Molina, F.J., Stow, D.A.V., Alvarez Zarkian, C.A., Expedition IODP 339 Scientists, 2013. IODP expedition 339 in the gulf of Cadiz and off west Iberia:

- decoding the environmental significance of the Mediterranean outflow water and its global influence. *Sci. Drill.* 16, 1–11.
- Hernández-Molina, F.J., Stow, D.A.V., Alvarez Zarikian, C.A., Acton, G., Bahr, A., Balestra, B., Ducassou, E., Flood, R., Flores, J.-A., Furota, S., Grunert, P., Hodell, D.A., Jimenez-Espejo, F., Kyoung, K.J., Kriesek, L., Kuroda, J., Li, B., Llave, E., Lofi, E., Lourens, L., Miller, M., Nanayama, F., Nishida, N., Richter, C., Roque, C., Pereira, H., Sanchez Goñi, M.F., Siero, F.J., Singh, A.D., Sloss, C., Takashimizu, Y., Tzanova, A., Voelker, A., Williams, T., Xuan, C., 2014. Onset of Mediterranean outflow into the north Atlantic. *Science* 344, 1244–1250.
- Iribarren, L., Vergés, J., Fernández, M., 2009. Sediment Supply from the Betic–Rif Orogen to Basins Through Neogene. *Tectonophysics, The geology of vertical movements of the lithosphere* 475, pp. 68–84.
- Jones, R.W., Brady, H.B., 1994. *The Challenger Foraminifera*. Oxford science publication (149 pp.).
- Jorissen, F.J., de Stigter, H.C., Widmark, J.G.V., 1995. A Conceptual Model Explaining Benthic Foraminiferal Microhabitats. *Mar. Micropaleontol.*, Selected papers from the Fifth International Symposium of Foraminifera 26, pp. 3–15.
- Jorissen, F.J., Witting, L., 1999. Ecological evidence from live-dead comparisons of benthic foraminiferal faunas off cape blanc (northwest Africa). *Palaeogeogr. Palaeoclimatol. Palaeoecol.* 149, 151–170.
- Kennett, J.P., Srinivasan, M.S., 1983. Neogene Planktonic Foraminifera: A Phylogenetic Atlas. Hutchinson and Ross, Pennsylvania (246 pp.).
- Khélifi, N., Samthein, M., Andersen, N., Blanz, T., Frank, M., Garbe-Schönberg, D., Haley, B.A., Stumpf, R., Weinelt, M., 2009. A major and long-term Pliocene intensification of the Mediterranean outflow, 3.5–3.3 Ma ago. *Geology* 37, 811–814.
- Kouwenhoven, T.J., 2000. Survival under stress : benthic foraminiferal patterns and Cenozoic biotic crises. *Geol. Ultraiect.* 186, 1–206.
- Lastras, G., Canals, M., Urgeles, R., De Batist, M., Calafat, A.M., Casamor, J.L., 2004. Characterisation of the recent BIC'95 debris flow deposit on the Ebro margin, western Mediterranean sea, after a variety of seismic reflection data. *Mar. Geol.* 213, 235–255.
- Ledesma, S.M., 2000. *Astrobiocronología y Estratigrafía de Alta Resolución del Neógeno de la Cuenca del Guadalquivir-Golfo de Cádiz* PhD Thesis University of Salamanca, Salamanca.
- Levy, A., Mathieu, R., Poignant, A., Rosset-Moulinier, M., Ubaldo, M.L., Lebreiro, S., 1995. Foraminifères actuels de la marge continentale portugaise-inventaire et distribution. *Mem. Inst. Geol. Min.* 32, 3–116.
- Llave, E., Schönfeld, J., Hernández-Molina, F.J., Mulder, T., Somoza, L., Díaz del Río, V., Sánchez-Almazo, I., 2006. High-resolution stratigraphy of the Mediterranean outflow contourite system in the gulf of Cadiz during the late Pleistocene: the impact of Heinrich events. *Mar. Geol.* 227, 241–262.
- Lourens, L.J., 2004. Revised tuning of ocean drilling program site 964 and KC01B (Mediterranean) and implications for the $\delta^{18}O$, tephra, calcareous nannofossil, and geomagnetic reversal chronologies of the past 1.1 Myr. *Paleoceanography* 19, PA3010.
- Lourens, L.J., Antonarakou, A., Hilgen, F.J., Van Hoof, A.A.M., Vergnaud-Grazzini, C., Zachariasse, W.J., 1996. Evaluation of the plio-pleistocene astronomical timescale. *Paleoceanography* 11, 391–413.
- Lutze, G.F., 1986. *Uvigerina* species of the eastern north Atlantic. *Utrecht Micropaleontol. Bull.* 22, 21–46.
- Major, J.J., Iverson, R.M., 1999. Debris-flows deposition: effects of pore-fluid pressure and friction concentrated at flow margins. *GSA Bull.* 111, 1424–1434.
- Maldonado, A., Nelson, C.H., 1999. Interaction of tectonic and depositional processes that control the evolution of the Iberian gulf of Cadiz margin. *Mar. Geol.* 155, 217–242.
- Maldonado, A., Somoza, L., Pallarés, L., 1999. The betic orogen and the Iberian–African boundary in the gulf of Cadiz: geological evolution (central north Atlantic). *Mar. Geol.* 155, 9–43.
- Marques da Silva, C., Landau, B., Domenech, R., Martinell, J., 2010. Pliocene Atlantic molluscan assemblages from the mondogo basin (Portugal): age and palaeoceanographic implications. *Palaeogeogr. Palaeoclimatol. Palaeoecol.* 285, 248–254.
- Martínez del Olmo, W., 2004. *La exploración de hidrocarburos en el terciario de España*. *Bol. Geol. Min.* 115, 411–426.
- Mathieu, R., 1986. *Sédiments et Foraminifères Actuels de la Marge Continentale Atlantique du Maroc* Unpublished Ph.D. Dissertation, Université Pierre et Marie Curie, Paris, France (420 pp.).
- Medialdea, T., Vegas, R., Somoza, L., Vázquez, J.T., Maldonado, A., Díaz del-Río, V., Maestro, A., Córdoba, D., Fernández-Puga, M.C., 2004. Structure and evolution of the "olistostrome" complex of the Gibraltar arc in the gulf of Cádiz (eastern central Atlantic): evidence from two long seismic cross-sections. *Mar. Geol.* 209, 173–198.
- Mendes, I., Gonzales, R., Dias, J.M.A., Lobo, P., Martins, V., 2004. Factors influencing recent benthic foraminifera distribution on the Guadiana shelf (southwestern Iberia). *Mar. Micropaleontol.* 51, 171–192.
- Mendes, I., Alveirinho Dias, J., Schönfeld, J., Ferreira, Ó., 2012. Distribution of living benthic foraminifera on the northern gulf of Cadiz continental shelf. *J. Foraminif. Res.* 42 (1), 18–38.
- Migeon, S., Ducassou, E., Le Gonidec, Y., Rouillard, P., Mascle, J., Revel-Rolland, M., 2010. Lobe construction and sand/mud segregation by turbidity currents and debris flows on the western Nile deep-sea fan (eastern Mediterranean). *Sediment. Geol.* 229, 127–143.
- Miller, K., Kominz, M., Browning, J., Wright, J., Mountain, G., Katz, M., Sugarman, P., Cramer, B., Christie-Blick, N., Pekar, S., 2005. The Phanerozoic record of global sea-level change. *Science* 310, 1293–1298.
- Mohrig, D., Wipple, K.X., Hondzo, M., Ellis, C., Parker, G., 1998. Hydroplaning of subaqueous debris flows. *Geol. Soc. Am. Bull.* 110, 387–394.
- Monegatti, P., Raffi, S., 2007. Mediterranean-middle eastern Atlantic façade: molluscan biogeography & ecobiostatigraphy throughout the late Neogene. *Açoreana Suppl.* 5, 126–139.
- Mulder, T., Alexander, J., 2001. The physical character of subaqueous sedimentary density flows and their deposits. *Sedimentology* 48, 269–299.
- Murat, A., 1999. Pliocene–Pleistocene Occurrence of Sapropels in the Western Mediterranean Sea and Their Relation to Eastern Mediterranean Sapropels. In: Zahn, R., Comas, M.C., Klaus, A. (Eds.), *Proceedings of the Ocean Drilling Program*. 161, pp. 519–527.
- Nelson, C.H., Baraza, J., Maldonado, A., 1993. Mediterranean undercurrent sandy contourites gulf of Cadiz, Spain. *Sediment. Geol.* 82, 103–131.
- Nelson, C.H., Baraza, J., Maldonado, A., Rodero, J., Escutia, C., Barber, J.H., 1999. Influence of the Atlantic inflow and Mediterranean outflow currents on late quaternary sedimentary facies of the gulf of Cadiz continental margin. *Mar. Geol.* 155 (1–2), 99–129.
- Noiva, J., Terrinha, P., Duarte, H., 2010. Alterações morfológicas do holocénico e tectónica recente ao largo de quarta, Algarve, sul de Portugal. VIII CNG 2010, 12.
- Raffi, I., Backman, J., Fornaciari, E., Pálke, H., Rio, D., Lourens, L., Hilgen, F., 2006. A review of calcareous nannofossil astrobiocronology encompassing the past 25 million Years. *Quat. Sci. Rev. Crit. Quat. Stratigr.* 25, 3113–3137.
- Rathburn, A.E., Corliss, B.H., 1994. The ecology of living (stained) deep-sea benthic foraminifera from the Sulu sea. *Paleoceanography* 9 (1), 87–150.
- Riaza, C., Martínez del Omo, W., 1996. Depositional model of the Guadalquivir-Gulf of Cadiz Tertiary basin. In: Friend, P., Dabrio, C. (Eds.), *Tertiary Basins of Spain: The Stratigraphic Record of Crustal Kinematics*. Cambridge University Press, pp. 330–338.
- Rodríguez-Lazaro, J., Ruiz-Muñoz, F., 2012. A General Introduction to Ostracods: Morphology, Distribution, Fossil Record and Applications. In: Horne, D.J., Holmes, J.A., Rodríguez-Lazaro, J., Viehberg, F.A. (Eds.), *Ostracoda as Proxies for Quaternary Climate Change* Developments in Quaternary Science 17. Elsevier, pp. 1–14.
- Rogerson, M., Rohling, E.J., Weaver, P.P.E., Murray, J.W., 2005. Glacial to interglacial changes in the settling depth of the Mediterranean outflow plume. *Paleoceanography* 20, 1–12.
- Roque, C., Duarte, H., Terrinha, P., Valadares, V., Noiva, J., Cachão, M., Ferreira, J., Legoinha, P., Zitellini, N., 2012. Pliocene and quaternary depositional model of the Algarve margin contourite drifts (gulf of Cadiz, SW Iberia): seismic architecture, tectonic control and paleoceanographic insights. *Mar. Geol.* 303–306, 42–62.
- Ruiz, F., Gonzalez-Regalado, M.L., 1996. Les ostracodes du golfe Mio-Pliocene du Sud-ouest de l'Espagne. *Rev. Micropaleontol.* 39 (2), 137–151.
- Ruiz-Muñoz, F., Gonzalez-Regalado, M.L., Munoz Pichardo, J.M., 1998. Análisis de poblaciones en ostracodos: el género *Urocythereis* en medios actuales y neógenos del SO de España. *Geobios* 31 (1), 61–74.
- Ruiz, F., González-Regalado, M.L., Abad, M., Civis, J., González Delgado, J.A., Mara García, E.X., Prudêncio, M.L., Dias, M.I., 2008. Pliocene ostracods of southwestern Europe. *Geobios* 41, 845–859.
- Schwab, W.C., Lee, H.J., Twichell, D.C., Locat, J., Nelson, C.H., McArthur, W.G., Kenyon, N.H., 1996. Sediment mass-flow processes on a depositional lobe, outer Mississippi fan. *J. Sediment. Res.* 66, 916–927.
- Siero, F.J., Ledesma, S., Flores, J.-A., Torrecusa, S., del Olmo, W.M., 2000. Sonic and gamma-ray astrochronology: cycle to cycle calibration of Atlantic climatic records to Mediterranean sapropels and astronomical oscillations. *Geology* 28, 695–698.
- Stefanelli, S., 2004. Cyclic changes in oxygenation based on foraminiferal microhabitats: early-middle Pleistocene, Lucania basin (southern Italy). *J. Micropaleontol.* 23, 81–95.
- Torelli, L., Sartori, R., Zitellini, N., 1997. The giant chaotic body in the Atlantic ocean off Gibraltar: new results from a deep seismic reflection survey. *Mar. Pet. Geol.* 14, 125–138.
- Van der Zwaan, G.J., Jorissen, F.J., De Stigter, H.C., 1990. The depth-dependency of planktonic/benthic foraminiferal ratios: constraints and applications. *Mar. Geol.* 95, 1–16.
- Van der Zwaan, G.J., Jorissen, F.J., 1991. Biofacial patterns in river-induced shelf anoxia. *Geol. Soc. Lond. Spec. Publ.* 58, 65–82.
- Van Hinsbergen, D.J.J., Kouwenhoven, T.J., Van der Zwaan, G.J., 2005. Paleobathymetry in the backstripping procedure: correction for oxygenation effects on depth estimates. *Palaeogeogr. Palaeoclimatol. Palaeoecol.* 221, 245–265.
- Van Morkhoven, F.P.C.M., 1986. Cenozoic Cosmopolitan Deep-Water Benthic Foraminifera. In: Henri, J. (Ed.), *Oertli. Elf Aquitaine* (421 pp.).
- Wright, B.R., Berggren, W.A., 1977. Paleocene and early Eocene of the Rio Grande and Tampico embayments: foraminiferal biostratigraphy and paleoecology. *Mar. Micropaleontol.* 2 (2), 67–103.
- Zitellini, N., Gracia, E., Matias, L., Terrinha, P., Abreu, M.A., DeAlteris, G., Henri, J.P., Dañobeitia, J.J., Masson, D.G., Mulder, T., Ramella, R., Somoza, L., Diez, S., 2009. The quest for the Africa-Eurasia plate boundary west of the strait of Gibraltar. *Earth Planet. Sci. Lett.* 280, 13–50.